The Compared Effects of Lithium Isotopes ^{6}Li and ^{7}Li on GSK-3-β Activity and the Biochemistry of HT22 Neuronal Cells

by

James Livingstone

A thesis

presented to the University of Waterloo

in fulfillment of the

thesis requirement for the degree of

Master of Science

in

Biology

Waterloo, Ontario, Canada, 2020

©James Livingstone 2020

Author's Declaration

This thesis consists of material all of which I authored or co-authored: see Statement of Contributions included in the thesis. This is a true copy of the thesis, including any required final revisions, as accepted by my examiners.

I understand that my thesis may be made electronically available to the public

Statement of Contributions

All work in this thesis was completed by me except for the following:

Kartar Singh made contributions to cell culture and treatment that would become Chapter 3.

The ICP-MS data presented in Chapter 5 and Appendix A was collected and analyzed by Dr. Brian Kendall, Dr. Chris Yakymchuk, and Sarah McChaugherty from samples prepared by me.

All data was processed by me and all figures were drawn by me.

Abstract

The use of lithium in treatment of mental illnesses like bipolar disorder, major depressive disorder, and schizophrenia dates to the mid 20th century. Some research also indicates that the symptoms of Alzheimer's Disease can be lessened by lithium treatment. But despite widespread use, the complete mechanisms through which lithium works are largely unknown. The "isotopically impure" lithium used to treat these disorders is comprised of approximately 7.59% ^{6}Li and 92.41% ^{7}Li, about the normal distribution of the lithium isotopes in nature. Pharmacologically, no distinction has been made between the two isotopes. However, preliminary animal model research suggests that these isotopes may have differential effects on the maternal behaviours of rats, while other cellular research has found a difference in the sustained concentration of each isotope in both neural cells and erythrocytes. The research presented here investigates the possibility that the isotopes ^{6}Li and ^{7}Li may have different effects on neuronal physiology and molecular processes. No significant difference was found on glycogen synthase kinase-3-β (GSK-3-β) activity, GSK-3-β phosphorylation rates in HT22 cells, or HT22 cell viability when treated with ^{6}Li and ^{7}Li. However, a possible difference has been found in the sustained lithium isotope concentrations across the HT22 plasma membrane. More research is needed to confirm and elucidate this global set of data, but the results presented here indicate a reasonable possibility that lithium isotopes are differentially fractionated across the HT22 plasma membrane.

Acknowledgements

There are many who were vital in the completion of this thesis. I would like to thank my supervisor Dr. Zoya Leonenko for her efforts in supporting me and all her students both in the lab and personally. Her patience while waiting on experimental results is unmatched. I am grateful for the chance to complete this thesis under her supervision.

I thank Dr. Michael Beazely for allowing me to complete all my work in his lab at the School of Pharmacy, for agreeing to be on my committee, and for providing invaluable guidance when needed.

I would like to thank Dr. David Spafford for agreeing to be on my committee.

I would also like to thank Dr. Michel Gingras for his advice, his role in bringing the ICP-MS experiments to reality, and his thought-provoking questions and comments.

My lab mate of the last two years, Morgan Robinson, has been an extremely knowledgeable colleague, a good friend, and a reliable fount of good ideas. I thank him for his willingness to sacrifice his time to teach and help me and other students.

Some of the work presented in this thesis was partially completed by Karter Singh. I thank him for his willingness to learn and contribute to both the lab and my thesis.

I thank Dr. Brian Kendall, Dr. Chris Yakymchuk and Sarah McChaugherty for working with me in the ICP-MS analyzation of HT22 cell samples.

I would also like to acknowledge the University of Waterloo for allowing me a place in this endless pursuit of knowledge.

Last but certainly not least, I would like to acknowledge my friends and family who have supported me during the long years of my university education. I could not have come this far without them, and I am forever in their debt.

Dedication

I would like to dedicate this thesis to my family. From a young age, they encouraged and supported me and my never-ending thirst for knowledge. I am who I am today only because of my family.

Table of Contents

List of Figures

Chapter 1

Chapter 2

Chapter 3

Chapter 4

Chapter 5

List of Tables

Chapter 2

List of Abbreviations

Adenosine Monophosphate (ADP)
Adenosine Triphosphate (ATP)
Alzheimer's Disease (AD)
Amyloid Precursor Protein (APP)
Analysis of Variance (ANOVA)
α-amino-3-hydroxy-5-methyl-4-isoxazolepropionic acid (AMPA)
Bicinchoninic Acid (BCA)
Bipolar Disease (BD)
Bovine Serum Albumin (BSA)
Brain-Derived Neurotrophic Factor (BDNF)
Deuterium Water (D_2O)
Dimethylthiazol Diphenyltetrazolium (MTT)
Ethylenediaminetetraacetic acid (EDTA)
Ethylene Glycol Tetraacetic acid (EGTA)
Fetal Bovine Serum (FBS)
Gamma-Aminobutyric Acid (GABA)
Glycogen Synthase Kinase-3-Beta (GSK-3-ß)
Glycogen Synthase Kinase-3-Beta Serine 9 (S9)
Glycogen Synthase Kinase-3-Beta Tyrosine 216 (TYR216)
Inductively Coupled Plasma Mass Spectrometry (ICP-MS)
Insulin Growth Factor 1/Mammalian Target of Rapamycin pathway (IGF1/mTOR pathway)
Mammalian target of rapamycin complex 1, 2 (mTORC1, 2)
Median Lethal Dose (LD50)
N-Methyl-D-Aspartate (NMDA)
Phosphoinositide-3 kinase (PI3K)
Protein Kinase A (PKA)
Phosphate-Buffered Saline (PBS)
Protein Kinase B (PKB)
Protein Kinase C (PKC)
Ras Homolog Enriched in Brain (RHEB)
Simian Virus 40 (SV40)
T-cell factor/lymphoid enhancer factor (TCF/LEF)
Tris-Buffered Saline Solution with 1% Tween (TBST)
TSC1/2 (tuberous sclerosis complex 1/2)
Wingless-related Integration site/Beta-catenin pathway (Wnt/β-catenin pathway)

Chapter 1 : Introduction

1.1 Lithium

Lithium (Li^+) is the smallest monovalent cation and is quite ubiquitous throughout the universe. It is present in variable amounts in rocks, soil, and water and is often ingested in low amounts by humans and animals[1]. It is also not well regulated by multicellular animals and in excess is acutely toxic, causing fatigue, nausea, tremors, and kidney failure[2]. On the other hand, based on experiments in which animals are deprived of lithium, it seems to be an essential micronutrient[3,4]. In human populations where lithium is naturally present in drinking water, there is a correlation between the increased lithium and decreased homicide, crime, dementia, and suicide[5].

Li^+ salts were first used in the 1870s as a treatment for gout and in the following years were used to treat mania and replace dietary table salt for those with hypertension and heart disease[6]. It was banned for a short while over concerns of side effects and deaths but by 1974, the United States approved lithium to treat bipolar disorder[6]. The specific mechanisms of action of Li^+ in stabilizing mood were completely unknown and still are to a large degree. Since then, there has been much research on the many effects of Li^+ on neuronal biochemical processes[7].

Similarities Between Lithium and Other Biologically Important Cations

As mentioned, Li^+ is relatively unique in that it is not strictly regulated by multicellular animals. Virtually every other ion that multicellular organisms encounter (H^+, Na^+, K^+, Ca^{2+}, Cl^-, Mg^{2+} etc.) is extremely well regulated by specialized membrane channels and active transporters. Li^+, even though it is very biologically active and quite toxic in sufficient

amounts, has no known dedicated channel or transporter. In fact, it seems that many of its effects work through its competition with these other ions for transporters, channels, and enzymatic sites.

Comparison between Li^+ and other cations would lead one to expect that Li^+ could compete effectively with Mg^{2+} due to similar hydrated ionic radii, and this hypothesis has been borne out as correct in many experimental observations. The effective ionic radius of Li^+ is 76 pm, quite close to Mg^{2+} at 72 pm[8]. Li^+ is also able to compete with Na^+ for channels, displacing Na^+ in many of its positions in the cell[9]. This principle of ionic competition seems to describe many Li^+ interactions with enzymes and bioactivity.

Lithium Bioactivity

The Li^+ concentration in blood plasma is almost directly proportional to Li^+ ingestion[10]. This simple observation serves to illuminate the concept that Li^+ is transported across biological membranes passively but is not well regulated.

One of the major avenues for Li^+ passage across cell membranes is through Na^+ channels. Both voltage-gated and non-voltage-gated Na^+ channels show approximately equal permeability to Na^+ and Li^+ [11]. In a study of a prokaryotic Na^+ channels, approximately equal permeabilities of Li^+ and Na^+ were revealed[12]. Li^+ is transported by the phloretin sensitive Na^+-Li^+ counter-transport system in the red blood cell[13]. The ability of the kidney to resorb Li^+ is largely due to the ability of the Na^+-P^+ cotransporter in the nephron proximal tubule to substitute Na^+ for Li^+ - without this reabsorption, Li^+ concentrations in the body would be much lower[14]. Li^+ can also be a substitute for Na^+ in the Na^+-aspartate cotransporter, though less effectively[15]. Li^+ efflux from cells also seems to be mostly Na^+ channel-dependent, and is due to Na^+-Li^+

counter-transport systems in which Li^+ competes with Na^+ [16] or protons[17]. In mitochondrial membranes, Li^+ has been found to protect neuronal mitochondria against elevated calcium, which might be mediated through the Na^+/Ca^{2+} exchanger by, once again, replacing Na^+ [18,19]. In all these mechanisms, Li^+ is transported through the cell non-specifically through channels and transporters meant for Na^+.

The competition of Li^+ with Na^+ decreases the influx of Na^+ in excitable cells, resulting in a slower rate of depolarization[20]. The overall resting membrane potential of neuronal cells is also modulated by Li^+ through activation of Na^+/K^+ pumps[21]. It has been theorized that part of the behaviour-modification seen in patients with bipolar disorder who are treated with lithium is due to lithium's ability to bring a hyperpolarized membrane potential back to normal resting potential[22].

Li^+ is also able to mimic and replace Mg^{2+} in many important biochemical mechanisms. Enzymatic kinase reactions are dependent on adenosine triphosphate (ATP) – the primary energy carrier in living organisms. In its biologically-active form, ATP is complexed with magnesium: Mg^{2+} forms ionic bonds with the O^- atoms bonded to either the α and β phosphates, or the β and γ phosphates[23]. This ATP-Mg complex is crucial in the function of enzymatic reactions that require ATP. Density functional calculations show that Li^+ can compete with Mg^{2+} in the ATP-Mg complex and in the metal-binding sites of enzymes[24,25]. Interestingly, these calculations indicate that each enzyme binding site shape itself influences whether Li^+ competes effectively with Mg^{2+}; this is the leading hypothesis for why Li^+ can directly inhibit some enzymes, but not others[24]. Li^+ therefore acts as a competitive inhibitor of many Mg^{2+}-dependant enzymes[26,27]. For example, Li^+ can inhibit β-adrenergic and muscarinic receptor coupling to G-

proteins by competing with Mg^{2+} [28] and can also substitute Mg^{+} as a cofactor in inositol monophosphatase, a critical molecular target for lithium treatment in bipolar disorder[29].

The ionic competition of Li^{+} with Mg^{2+} and Na^{+} has been proposed as the underlying and ultimate basis for the many effects of Li^{+} on animal cells[30]. The resulting effects are far-reaching and numerous, including many ATP-dependant reactions and cell metabolism-regulating mechanisms.

1.2 Lithium in the Treatment of Bipolar Disorder and Neurodegenerative Diseases

Lithium was approved to treat bipolar disorder (BD) by the FDA in 1974 before many of the underlying mechanisms of action were discovered[6]. Even now, with the general understanding of Li^{+} competition with Na^{+} and Mg^{2+}, the many biochemical effects within the cell are not completely elucidated. Understanding of the specific biochemical cascades and regulatory pathways that lithium affects is crucial to the understanding of the overall modulation of neuronal aspects by lithium.

Intracellular Cascades Vital to Cellular Regulation

Presented here are two pathways of cellular regulation that are modulated by lithium: the IGF1/mTOR (Insulin Growth Factor 1/Mammalian Target of Rapamycin) and the Wnt/β-catenin (Wingless-related Integration site/Beta-catenin) pathways. These are not the only pathways affected by lithium. However, these pathways have been implicated in both Alzheimer's disease (AD) and BD and have also been shown to be modulated by lithium, providing a useful framework within which the effects of lithium can be understood in the context of modern neurodegenerative disease treatment.

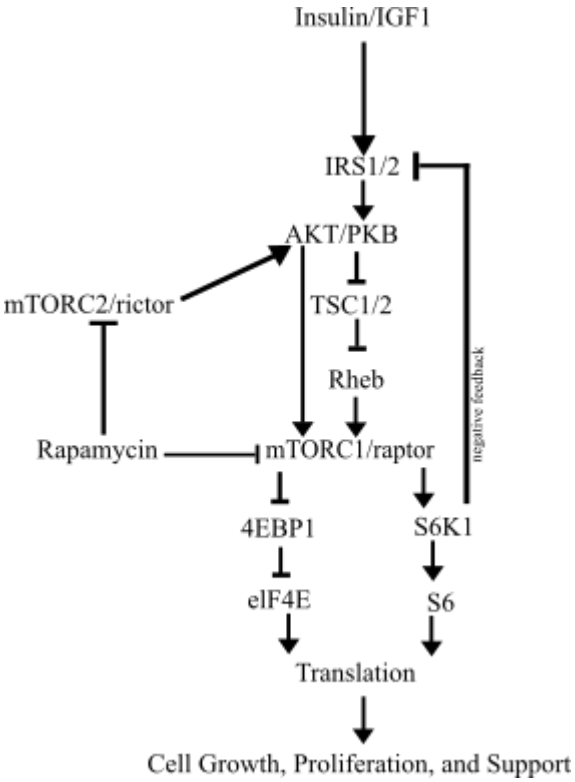

Figure 1-1: The IGF1/mTOR Pathway. *Generally, the IGF1/mTOR pathways signal for cell growth and division in response to nutrients and growth factors. Binding of IGF-1 or insulin to its receptor on the cell surface results in downstream intracellular activation of protein kinase B (PKB, also called AKT) and eventual activation of mTOR complex 1 (mTORC1). The mTORC1 then localizes to the lysosome to upregulate translation and protein synthesis through activation of translation initiation factors like EIF4E and ribosomal proteins like S6.*

The IGF1/mTOR pathway is vital to the survival and growth of normal cells through its promotion of generally proliferative processes[31]. The mTOR complexes 1 and 2 were first discovered through the characterization of a bacteria-derived compound called rapamycin. Rapamycin, an antifungal, also has impressive immunosuppressive and antitumor properties which are a result of its ability to inhibit the mTOR complexes 1 and 2 (figure 1-1)[32,33,34]. There are extensive cell regulation pathways surrounding mTORC1 and mTORC2 not shown in figure 1-1, but this simplified pathway serves to illustrate the general intracellular regulation of growth and support[35]. Dysfunction of these pathways is implicated in cancer genesis and progression[36], aging[37], and some degenerative diseases like AD[38].

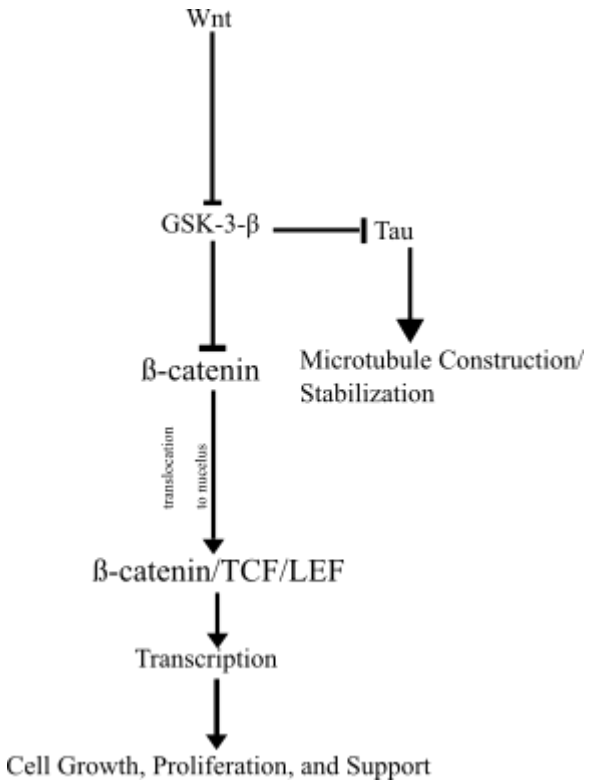

Figure 1-2: The Wnt/B-catenin Pathway*: Shown here in figure 1-2 is the canonical Wnt/β-catenin pathway. Signal transduction begins with the binding of the Wnt-protein ligand to a cell surface receptor of the Frizzled family which then transduces the signal through the Dishevelled protein into the cell. The Wnt/β-catenin canonical pathway results in activated GSK-3-β, accumulation of β-catenin and ultimately upregulation of cell-supporting gene transcription in the nucleus.*

The canonical Wnt/β-catenin pathway is one of three characterized Wnt receptor-based regulatory pathways. Much of the research that led to characterization of the Wnt pathways was first done in *Drosophila melanogaster* (the common fruit fly) but the Wnt pathway is evolutionarily conserved throughout the animal kingdom, including in mammals. The canonical Wnt/β-catenin pathway is involved in regulation of cell-supporting gene transcription and its dysfunction is associated with cancers[39], AD[40,41], and BD[42].

The insulin/mTOR and Wnt/β-catenin pathways share a particularly important kinase called glycogen synthase kinase-3-β (GSK-3-β). There are two types of GSK-3: GSK-3-β and GSK-3-α, both with similar roles in the cell. We will be examining GSK-3-β. GSK-3-β is a

regulatory kinase of over 100 different proteins and is important in healthy neuronal cell energy metabolism and development pathways[43,44]. GSK-3-β dysfunction is also implicated in many diseases including AD[45], type 2 diabetes[46], bipolar disorder[47], and some forms of cancer[48]. GSK-3-β is generally inhibited by Wnt, and generally inhibits mTOR (refer to Figure 1-3).

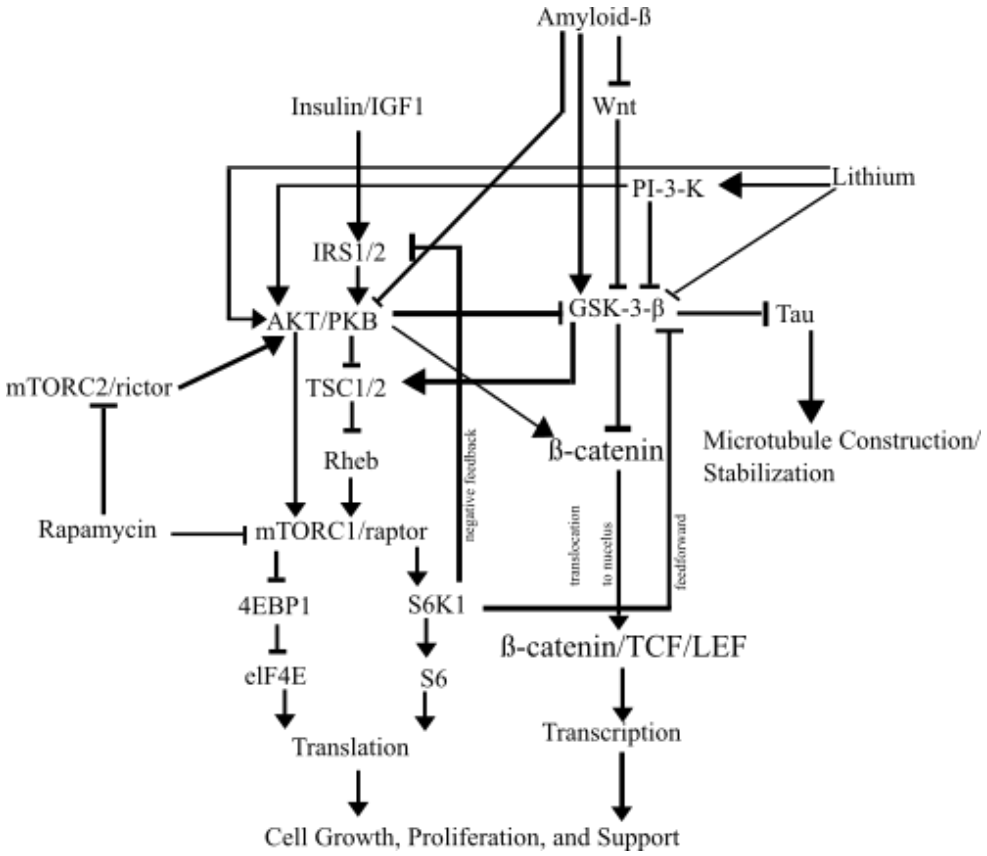

Figure 1-3: IGF1/mTOR and Wnt/B-catenin Pathways [49,50,51,52]. *Figure 1-3 illustrates a summarized fraction of the intracellular canonical pathways, allowing for visualization of the central role of GSK-3-β and the general effect of lithium. Overactivation of GSK-3-β can downregulate neurotrophic transcription and degrade the ability of tau to support microtubules, but also contribute to future and chronic mTORC1 under-activation and Wnt-targeted transcription suppression. There seems to be a possibility for intracellular feedforward and feedback loops that continually contribute to GSK-3-β activation, reminiscent of 'The GSK-3-β Hypothesis of Alzheimer's Disease'. The oligomeric form of amyloid-ß interacts with the insulin/AKT/mTOR pathway in both its physiological and pathological concentrations and forms*[49]*. Amyloid-β has even been shown to bind and inhibit Frizzled (the receptor to Wnt)*[53]*. This Wnt suppression can again induce more amyloidogenic processing*[54]*. Lithium is able to directly and indirectly reduce the overactivity of GSK-3-β, restoring function to tau and upregulating cell supporting processes.*

Intracellular Factors Involved in Alzheimer's Disease

First characterized by Dr. Alois Alzheimer, Alzheimer's Disease (AD) is marked by progressive symptoms of dementia, cognitive decline, and eventual death[55]. Some of the many causative suspects of AD include genetic factors[56], lifestyle[57], and chronic inflammation due to trauma[58] or low-level infection[59]. These challenges are thought to lead to accumulation of amyloid-ß plaques, fibrils, and oligomers that cause toxic effects to the neuron and eventually cell death[60].

The accumulation of amyloid-ß in the brain has been intensely studied as the cause of AD for decades. As such, the "amyloid cascade hypothesis" has been the leading framework within which most of the research has been conducted[60]. Much effort has gone towards developing drugs that lower the amyloid-ß load within the brain by increasing clearance, decreasing production, or preventing aggregation in an attempt to minimize and reverse the neurological damage[61,62]. Earlier research was mostly focused on plaques – insoluble aggregates postulated to cause toxicity, but the correlation between amyloid-ß plaque accumulation and degeneration is weak in humans and model animals. In fact, in AD model mice, high amounts of amyloid-ß plaques do not seem to cause neurologic degeneration or cognitive decline[63]. Similarly, there have been many human patients with high amounts of amyloid-ß plaques accumulation with no documented cognitive decline and also patients with the symptoms of AD but no amyloid-ß accumulation[64]. Amyloid-β oligomers are now considered by many to be the most toxic of the forms with mechanisms of neuronal disruption that include membrane oxidation, synaptic interaction, and receptor interaction[65].

There are also some mouse models that found no correlation between oligomer introduction and neurodegeneration[66], but others have found a strong correlation[67,68]. Some

researchers go so far as to suggest that amyloid-ß deposition and AD are unrelated, placing the blame mostly on tau-mediated injury[69], and tau-dependant pathways of neurodegradation has been characterized in AD mouse models[70]. It seems, as Musiek and Holtzman state, that amyloid-ß may be necessary but not sufficient to cause the neurodegeneration and cognitive decline of AD; perhaps amyloid-ß is only an early initiator of pathogenic cascades[71].

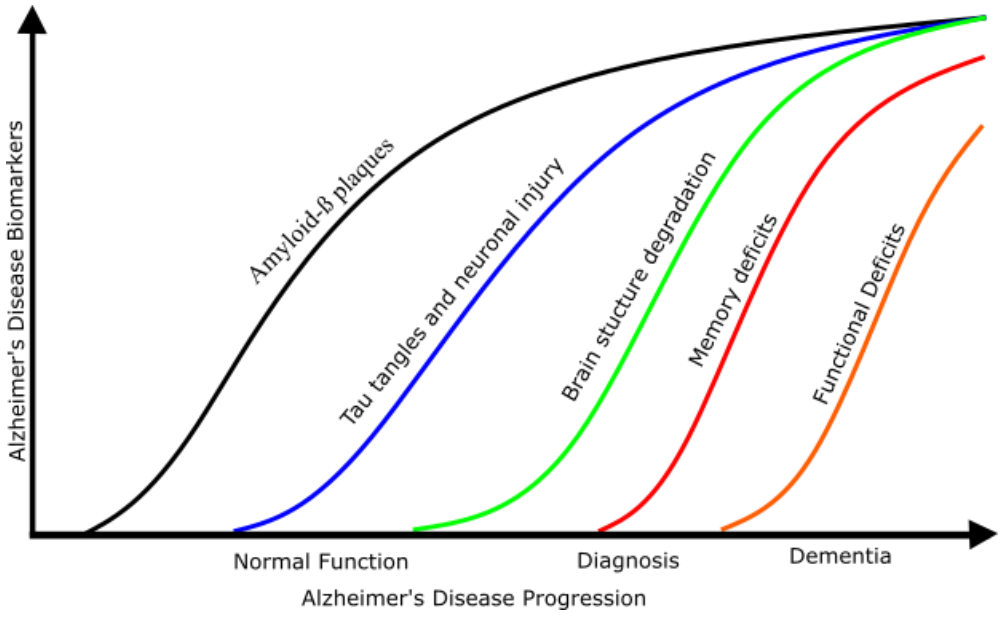

Figure 1-4: Biomarkers for the Progression of Alzheimer's Disease. *Clinical progression of AD can be difficult to detect in its early stages as there is a continuum between what is considered normal aging and AD dementia. Figure 1-4 shows the general progression of biomarkers correlated with AD as cognitive decline continues[72]. Unfortunately, a diagnostic test for AD is still unavailable and the only conclusive way to confirm AD is by detection of biomarkers by postmortem autopsy[73].*

The "GSK-3-β Hypothesis of Alzheimer's Disease" describes the possibility that overactivity of GSK-3-β may account for Tau hyperphosphorylation, increased amyloid-β production, and associated inflammatory responses[45,74,75]. GSK-3-β activity is regulated mostly by the phosphorylation states of Serine 9 (S9) and Tyrosine 216 (TYR216)[76]. S9 phosphorylation is known to inhibit its activity, while TYR216 phosphorylation is known to

increase its activity[77]. The S9 site is phosphorylated by AKT (Protein Kinase B - PKB)[78], Protein Kinase A (PKA)[79], Phosphoinositide 3-kinases (Pi-3-K)[80], and Protein Kinase C (PKC)[81] (Figure 1-3). The overactivity of GSK-3-β is hard to quantify in post-mortem humans, so the direct evidence for its overactivity is lacking. However indirect evidence of GSK-3-β overactivity in Alzheimer's disease (AD) does exist[82]. GSK-3-β has been shown to co-localize with neurofibril tangles[83]. There is increased GSK-3-β activity in the frontal cortex in those with AD[84], GSK-3-β is also upregulated in the hippocampus of AD-patients[85]. GSK-3-β is also a key mediator of apoptosis, dysregulation of which may account for some of the neuronal loss in AD[86]. GSK-3-β overactivity is also implicated in other brain disorders including schizophrenia[87] and Huntingtons Disease[88,89].

Lithium Effects within the Neuron

Lithium treatment is able to affect several aspects of cell molecular biology discussed. There is some evidence that the symptoms of AD can be lessened by lithium treatment, although AD is not an approved treatment currently[90]. Lithium can decrease the γ-cleavage of amyloid-ß from the amyloid precursor protein, reducing tau hyperphosphorylation and the severity of AD-like symptoms in model mice[91], but whether lithium decreases the overall amyloid-ß level in the brain is a matter of debate[92]. Many of lithium's effects within the cell act through kinase cascades - factors such as protein kinase B (PKB) and phosphoinositide-3 kinase (PI3K), among others[7]. These effects are widespread and seem to converge upon GSK-3-β (Figure 1-3). Lithium consequently can reduce GSK-3-β activity and reduce the hyperphosphorylation of Tau that causes microtubule instability and cytoskeletal collapse seen

in AD[92,93]. GSK-3-β can be both indirectly inhibited in the cell by the previously discussed kinases but can also be directly inhibited by Li^+ through Mg^{2+} competition.

There are several other cellular effects of lithium that may also contribute to its role in AD. Lithium is able to mimic Wnt signalling through its inhibition of GSK-3-β which promotes survival of post-mitotic neurons against amyloid-β toxicity, recovering β-catenin to normal levels (Figure 1-3)[94]. Lithium can upregulate neurotrophins like nerve growth factor, neurotrophin-3 and brain-derived neurotrophic factor[95]. Lithium also stimulates proliferation of stem cells, including bone marrow and neural stem cells in the subventricular zone, striatum, and forebrain through GSK-3-β-dependant Wnt/β-catenin activation[96,97].

The overall effects by lithium serve to decrease apoptosis, decrease glutamatergic sensitivity, improve cognitive functions, increase synaptic formation and increase neurogenesis – especially in the hippocampus[50,98,99,100]. These effects may disrupt the possible feedback mechanisms involved in keeping GSK-3-β activated and cell support downregulated in neurodegenerative disease.

Lithium in the Treatment of Bipolar Disorder

First described by Jean-Pierre Falret in the 1850s, bipolar disorders, then called “circular insanity”, are chronic, cyclic, and relatively common[101]. They are characterized by abnormally elevated and depressed moods often accompanied with psychosis. Approximately 4.8% of adults meet the criteria for one of Bipolar I, Bipolar II, Cyclothymic Disorder (Cyclothymia), and Bipolar Spectrum Disorder in their lifetime[102]. All these classifications involve changes in mood and activity levels in a cyclic nature, ranging from mild to severe. These disorders differ from major depression and other affective disorders in that the subject experiences manic episodes in

addition to depressive episodes. The classifications of bipolar disorders (BD) depend generally on the severity of the symptoms experienced. Those with bipolar spectrum disorders experience manic episodes that may present as extreme overconfidence, disinhibition, a decreased need for sleep, and a highly elevated mood. The patient also experiences periods of major depression[103].

BD is not significantly associated with any race, sex, or locale of living – though there is a higher rate of BD in those who are unmarried. The strongest predictor of BD is genetics. Genetic studies indicate that there is a highly heritable component with concordant rates of 57% between identical twins and 14% for fraternal twins[104]. Family members of the bipolar proband (the person diagnosed with the disorder) have between a 2.9% to 14.5% chance of also having BD and between a 4.2% to 24.3% chance of having a unipolar disorder[104].

Some researchers have suggested that GSK-3-β dysfunction may be the culprit for possible neuronal degradation seen in those with BD[105,106] and this degradation has caused some to consider BD as a neurodegenerative disease, though this opinion is relatively unsupported as yet in the overall literature[107]. Increased activity of GSK-3-β in BD may cause enhanced expression of inflammatory mediators, undermine neurogenesis and neuroprotection, and decrease effective regulation of glutamatergic signalling[42,105]. Single nucleotide polymorphisms in the GSK-3-β −50T/C and −1727A/T genes are also correlated with lithium non-responders – those patients for whom lithium does not provide effective treatment[108].

The discovery of pharmacological treatments for depression and mania revealed that bioamine neurotransmitter systems are heavily implicated in the pathophysiology of BD. These neurotransmitter systems are involved in the regulation of sleep, appetite, arousal, endocrine function, and emotional states[109]. Generally, the cell bodies of neurons in these neuroregulatory systems originate in the midbrain and project to all other areas of the brain, exerting their

regulatory effects. Lithium is usually the first medication prescribed to treat those with BD and is effective for approximately a third of patients[110]. Lithium affects many pathways within the brain and exerts many changes across the various neuron types. The noradrenergic, dopaminergic, serotonergic, cholinergic, and gamma-aminobutyric acid (GABA)ergic neuroregulatory systems have all been shown to be affected by lithium treatment as described below[109].

The noradrenergic system is strongly correlated with arousal level and is a key excitatory regulator of virtually all the brain regions. In those with BD, high levels of noradrenaline activity are correlated with mania, and low levels and correlated with depressive states[111]. Some genetic studies have suggested that polymorphisms of amine metabolic enzymes could contribute to bipolar symptomology through alteration of amine degradation rates[112-113]. Lithium has been shown to increase noradrenaline uptake at the synapse[114] and decrease the adrenergic receptor density at the synapse[115]. The overall reduction of noradrenergic signalling by lithium seems to have the effect of reducing the severity and duration of the manic state[43].

The dopaminergic system can be either excitatory or inhibitory depending on the types of receptors receiving innervation[116]. The “dopamine hypothesis” describes the possibility that abnormal dopaminergic neuron activity is a culprit of mood disorders like bipolar disorder[117]. This hypothesis has been developed to describe how faulty homeostatic mechanisms within the dopaminergic system may result in overcompensation with incorrect dopamine production, leading to cyclic switching from depression to mania and back[117]. GSK-3-β inhibitors like lithium have been shown to reduce D2 receptors through a GSK-3-β pathway in rats, resulting in the inhibitory effects of dopamine being enhanced[118]. Lithium has been shown to decrease overall excitatory neurotransmission through dopaminergic systems[119].

Serotonergic system functioning has been found to be decreased in those in a major depressive state based on serotonergic 5HT1A receptor agonist binding[120]. Lithium seems to increase the synthesis of serotonin in presynaptic neurons partly by increasing the uptake of the precursor tryptophan[121]. Lithium also increases serotonergic binding to the 1A receptor and decreases the reuptake of serotonin, increasing the effective amount of serotonergic signalling[114]. The net result is an increase in serotonergic neuro-modulatory system activity which has a dampening effect on the other excitatory neuro-modulatory systems like the noradrenergic[122].

In those with BD, it has been found that the cholinergic system activity is also well correlated with manic and depressive states. Decreased cholinergic activity is associated with mania, and increased activity is associated with depression[123]. Lithium is able affect this system: in mice studies lithium is able to increase acetylcholine synthesis in the striatum, cortex, and hippocampus of the mouse brain[124]. Even after induced "behavioural despair" caused by acetylcholinesterase inhibitors, lithium was able to mostly attenuate those behaviours[125].

The main inhibitory neurons in the brain – the GABAergic neurons, are also affected by lithium treatment. Neurons using the GABA neurotransmitter play a role in inhibiting dopamine and glutamate neurotransmission. Those with BD seem to have lower $GABA_B$ receptor levels[126]. Lithium can upregulate the $GABA_B$ receptor expression and facilitate GABA release to increase the overall inhibitory effect of GABA neurotransmission[126,127,128].

Lithium is able to decrease manic symptoms, depressive symptoms, and suicide rates to stabilize the long-term mood of about a third of patients with BD[129,130]. Lithium has been shown to increase cellular neuroprotection by increased production of neuroprotective proteins like brain derived neurotrophic factor, and has also been shown to promote

neuroproliferation[131,132,133]. Lithium has the overall effect of inhibiting excitatory neurotransmission and promoting inhibitory transmission to result in a tempering effect on mood in those with BD.

1.3 Isotopic Effects, Rat Maternal Behaviour, and the Quantum Brain

Lithium exists as two stable isotopes. The vast majority of research on lithium, including all previously mentioned, has been done using "isotopically impure" or "natural" lithium consisting of approximately 7.59% ^{6}Li and 92.41% ^{7}Li[134]. As such, it is unknown if each of the varied biochemical effects of lithium on neuronal cells is due to only one or both isotopes. ^{6}Li has a molecular weight of 6.015 g/mol and a quantum spin of 1, while ^{7}Li has a molecular weight of 7.016 g/mol and a quantum spin of 3/2. The two isotopes differ by about 14% in mass, 1 neutron, and their quantum spin.

So far, very little research has been conducted on the possible differential effects of lithium isotopes on molecular processes in the cell. Studies conducted decades ago found that ^{6}Li-treated mothers groomed and nursed their pups much more than ^{7}Li-treated mothers[135]. The median lethal dose (LD50) of ^{6}Li was found to be 13 meq/kg while the LD50 of ^{7}Li was 16 meq/kg in mice[136], though this finding has been challenged and no difference in mouse mortality was found by others[137]. The general activity level of the ^{6}Li - treated rats was found to be 50% lower than the ^{7}Li-treated rats at the same dose, though the methodology of these trials could be improved upon[138]. These same studies also found that ^{6}Li concentrations were increased by 25% compared to ^{7}Li in the erythrocytes, suggesting that the erythrocyte membrane has the capability of distinguishing between the two isotopes[138]. It was also reported that neurons in the rat cerebral cortex will sustain 50% higher ^{6}Li concentrations than ^{7}Li when

an equal dose of each is administered, possibly due to different uptake efficiencies[139]. These findings suggest, despite issues with methodology and replicability, that there is a significant difference between the effects of lithium isotopes on mammalian neuronal physiology.

A significant isotopic effect is within the realm of possibility and has precedent. For example, "heavy" water (D_2O), is water in which the hydrogen proton is replaced with its heavier isotope deuterium. The differences in hydrogen bond energy and length for D_2O are significant, resulting in changes in many chemical behaviours. D_2O is 10.6% heavier than H_2O and is slightly toxic to eukaryotes[140]. The hydrogen bonds between D_2O molecules are stronger, which results in disruption of normal enzymatic reactions in cells – particularly in the assemblies of the mitotic spindle necessary for cell division in eukaryotes[141,142]. A 25% substitution of H_2O with D_2O within eukaryotes results in problems with cell division and a 50% substitution usually results in death[143].

There are several ways through which quantum effects change reaction rates in general. Kinetic isotope effects are seen throughout the natural world and are phenomena in which isotopes exhibit different reaction rates[144]. Heavier isotopes of Mg^{2+} are often preferentially taken up by plants[145], while the lighter ^{12}C isotope is preferentially taken up in photosynthesis[146]. Often, lighter isotopes are more reactive because heavier isotopes have lower vibrational frequencies (and thus a smaller zero-point energy), implying a greater energetic input needed to reach the transition state and consequently causing a slower reaction rate[147]. This effect is most drastic in lighter atoms and becomes almost negligible in larger atoms when the isotopic mass difference is a small percentage of overall mass.

Quantum tunneling is another possible way by which isotopes can exhibit differential effects. When a particle wavefunction spreads across the space of a potential barrier, the particle

has a non-zero probability of "existing" (e.g. being detected) on the other side of that barrier – quantum tunneling. In this way, particles can propagate through a potential barrier by means not predicted by classical mechanics. These effects are documented for electrons and protons in many biological processes such as photosynthesis and cellular respiration[148]. Recently, quantum tunneling of Li^+ through closed Na^+ channels has been calculated as possible[149,150]. It could be that ^6Li, being less massive, may more readily tunnel through these channels than ^7Li. In a similar vein, it has also been calculated that Mg^{2+} may depolarize the neuronal membrane by quantum tunneling through closed channels[151]. These hypotheses are yet to be experimentally tested.

There are some who believe the different nuclear quantum spins of the lithium isotopes could have effects on proposed "quantum processing" in the brain through entanglement between Posner molecules[152]. These Posner molecules $Ca_9(PO_4)_6$ consist of phosphate and calcium atoms interacting in such a way that their spins can become entangled – possibly for up to 37min in normal physiological conditions[153]. Multiple entangled Posner molecules have been suggested to trigger cross-correlated release of Ca^{2+} within the cell upon disentanglement, enhancing the probability of neuronal depolarization[154]. More recent research has indicated that ^6Li may be more effective than ^7Li in suppression of ketamine-induced hyperactivity in a rat model of mania[155]. Perhaps more surprisingly, it has recently even been observed that nuclear spin may affect the anesthetic properties of xenon isotopes in mice[156]. If lithium isotopes do indeed have differential effects on the neuronal cell, perhaps the possibility of these hypotheses would increase beyond current speculation.

1.4 The Immortal Neuron

In-vitro research into neuronal cell processes is often accomplished using immortalized cell lines. These cell lines are derived from cells extracted from animals and humans that have been manipulated to be "immortal" - to undergo mitotic division continuously. Some of these cell lines, such as HeLa cells, were derived from natural cancers already mutated[157]. Many cell lines are immortalized through exogenous expression of telomerase reverse transcriptase to extend telomeres and avoid replicative senescence[158]. Other cells are immortalized through the use of simian virus 40 (SV40)[159].

The HT22 neuronal cell line is glutamate-sensitive and was subcloned from the HT4 line, originally derived from the mouse hippocampus through SV40 T-antigen immortalization[160,161,162]. The hippocampus is involved in normal brain cognition, learning, and memory and is also one of the first structures that becomes noticeably degraded in those afflicted with AD[163]. These HT22 cells are increasingly being used for study into processes involving glutamate and acetylcholine toxicity. Neurodegenerative diseases such as Parkinson's, Alzheimer's, and Huntington's all seem to involve glutamate toxicity in some way and HT22 cells have been used in the study of each[161,164].

While the literature correctly identifies HT22 cells as a glutamate-sensitive line, these cells require specific differentiation to express this quality – something that some have overlooked. In their undifferentiated exponential-growth state, HT22 cells seem to express virtually no N-Methyl-D-Aspartate (NMDA) receptors nor any cholinergic receptors and seem to be glutamate-sensitive only through oxidative stress pathways[161]. When HT22 cells are properly differentiated, their sensitivity to glutamate increases by approximately two orders of magnitude, and this toxicity can be rescued by treating with NMDA receptor antagonists[161]. In this research,

differentiation of HT22 cells was accomplished by incubation for 24h in neurobasal media supplemented with 5mM N2 supplement and 5mM L-glutamine before treatment with lithium. This differentiation is crucial to ensure the HT22 cells exhibit more mature excitatory neuronal-like profiles.

However, this differentiation can also alter other cellular signalling pathways and cellular attributes. While neurobasal media is a mainstay in many labs for the reasons already mentioned, there is some research that indicates it may be responsible for cell death from induced excitotoxicity in primary rat neuronal cells[165]. This toxicity is mediated by the apparent large amounts of L-cystine (260uM) that are able to induce excitotoxicity through activation of NMDA receptors[165]. The question of whether neurobasal is contributing to HT22 excitotoxicity is yet unanswered, especially since the HT22 cells seem to not express NMDA receptors before differentiation. While some might see these findings as indications that the neurobasal media model is unsuitable for investigations into NMDA-mediated effects, the literature demonstrates clear evidence that neurobasal does not inhibit NMDA-mediated toxicity caused by glutamate treatment in HT22 cells[161]. Thus, differentiation by neurobasal media was used in this research with consideration for the possible effect of excitotoxicity.

Overall, the use of the HT22 cell line is advantageous due to quick doubling time and hardy constitution. The ability to differentiate the cells into an acceptable excitatory model is invaluable, allowing a reasonable approximation of the excitatory glutamate-sensitive neurons found in the hippocampus.

1.5 Research Goal and Experimental Objectives

Research Goal: the overall purpose of this research was to determine if there is a differential effect between the two lithium isotopes ^{6}Li and ^{7}Li on neuronal-like cell qualities. Four separate classes of experiments were conducted with this goal in mind.

Objective 1: the lithium isotope fractionation by the neuron plasma membrane was examined to determine if lithium isotopes are fractionated at different rates across the plasma membrane.

Objective 2: the toxicity of lithium isotopes in HT22 cells was examined to determine if the lithium isotopes have different toxicity levels *in-vitro* in HT22 cells that are both undifferentiated and differentiated by neurobasal media.

Objective 3: direct lithium isotope inhibition of GSK-3-β kinase activity was measured to determine if the lithium isotopes directly inhibit GSK-3-β kinase activity at different rates.

Objective 4: lithium's effects on GSK-3-β phosphorylation was measured to determine if lithium isotope treatment on HT22 cells results in differential phosphorylation rates of the GSK-3-β S9 site.

These four classes of experiments cover quite a large area of research and all of them are but the first forays into their respective domains. There is quite a bit more work to be completed before overall definitive conclusions can be drawn, but the data presented here gives a reasonable basis for an isotopic effect across the plasma membrane and indicates that further research into the differential effects of lithium isotopes is warranted.

Chapter 2 : Lithium Isotope Fractionation by the Neuron Plasma Membrane

2.1 Objectives and Hypotheses

The question as to whether the lithium isotopes are differentially fractionated across the plasma membrane is perhaps one of the most important within this research. Lithium is transported through Na^+ channels, and Na^+ channels are fundamental to the maintenance of the membrane potential and the workings of excitable cells. The only known research on the fractionation of lithium isotopes across the cell membrane indicate that there is an approximate 25% increase in ^6Li compared to ^7Li in the rat cortex after oral treatment[139]. A significant difference between lithium isotope concentration across the plasma membrane would suggest the hypothesis that the 14% mass difference is large enough for ion transporters to discriminate, and would provide definite plausibility to the hypothesis that the isotopes have a differential effect on cellular electrophysiology. Based on the previous findings, it was hypothesized that there would be a difference between the fractionation rates of lithium isotopes by the HT22 plasma membrane.

2.2 Materials and Methods - Inductively Coupled Plasma Mass Spectrometry (ICP-MS)

The protocols used in this experiment were developed with the help of Dr. Brian Kendal and Dr. Chris Yakymchuk at the University of Waterloo specifically for the purpose of answering the question as to whether the intracellular $^6Li/^7Li$ ratio of a live, intact neuron is different from the extracellular $^6Li/^7Li$ ratio. Even though the original reason for this first foray into ICP-MS analysis was to simply confirm that the techniques produce samples that contain lithium concentration within the ICP-MS detection range, exciting preliminary data concerning

the fractionation of lithium isotopes across the cell membrane was also obtained. After this experimental design was conceived, the article "Metal ion transport quantified by ICP-MS in intact cells" was used to guide further protocol optimization[166].

The Inductively Coupled Plasma Mass Spectrometer

Inductively coupled plasma mass spectrometry is used to detect atoms in an ionized sample. The sample is ionized by inductively coupled plasma, then the ions are separated in the mass spectrometer based on their mass-to-charge ratio (*m/z*) and a detector produces a signal from the separated ions. This detection is so sensitive that it can quantitatively detect isotopes to concentrations into the part-per-billion range[167]. Figure 2-1 illustrates a simple quadrupole ICP-MS schematic.

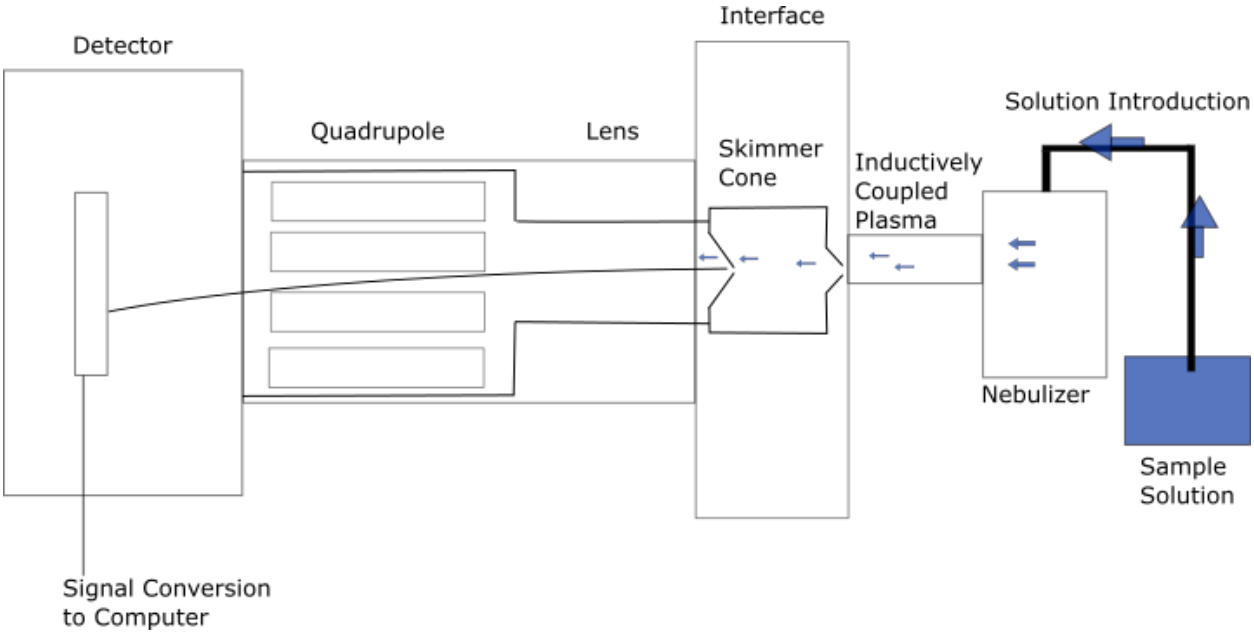

Figure 2-1: Diagram of a Quadrupole ICP-MS[168]***.*** *There are six basic parts of a quadrupole ICP-MS machine: the sample induction system, inductively coupled plasma, the interface, ion optics, quadrupole mass analyzer, and detector. The liquid samples are first nebulized to create a fine aerosol that is then introduced to argon plasma. The high temperature plasma atomizes and ionizes the sample, and the ions are guided through the interface region to the ion optics. The ion optics focuses the ion beam through the quadrupole mass analyzer. This mass analyzer separates the ions according to their m/z ratio. Only ions with a certain m/z ratio will reach the detector for a given voltage across the mass analyzer, the other ions will have unstable trajectories and collide with the mass analyzer*

walls before reaching the detector. Thus, the atomic profile can be analyzed by the m/z ratio data corresponding to the voltage ratio across the mass analyzer.

Sample Preparation

The preparation of cell homogenate to be analyzed was the most important aspect of this experiment. It was unknown whether the sample preparation techniques would be sufficient to allow fully independent analyzation of the extracellular media and intracellular cytoplasm. With this in mind, two plate sizes were used to grow the cells (6-well plates and 10 cm^2 plates) and two cell-harvesting techniques (trypsin and lysis buffer) were employed to give enough data to determine which techniques were acceptable.

Trypsin Harvesting

The technique of harvesting with trypsin involves removal of the media, washing with 2 mL of phosphate-buffered saline (PBS) twice, adding 100 uL of trypsin to each well to degrade the extracellular matrix holding the cells to the plate, then suspending the cells in 1 mL of full growth media. This technique results in whole cells being suspended in the media.

Lysis Buffer Harvesting

The technique of harvesting with lysis buffer is advantageous because it allows the semi-quantification of cell number by bicinchoninic acid (BCA) protein analysis. This technique is also almost identical to what is used for western blotting sample preparation as described in chapter 4. After removal of media, the wells were washed with 2mL of PBS twice, then 70 uL of lysis buffer was added [20 mM Tris-HCl pH 7.5, 150 mM NaCl, 1 mM Ethylenediaminetetraacetic acid (EDTA), 1 mM ethylene glycol tetraacetic acid (EGTA), 30 mM sodium pyrophosphate, 1 mM betaglycerophosphate, 1 mM sodium orthovanadate (Na3VO4),

and 1% triton]. The cells were scraped off the plate and homogenized using fine-gauge syringe needles. After centrifugation at 14,000 g at 4 C for 20 min, the supernatant was obtained and a BCA was performed, then it was suspended in 1 mL of media, and stored in -20 C until taken to the ICP-MS for analysis. This technique results in most of the plasma membrane being removed from the fraction.

6-Well Plates

HT22 cells were cultured in full growth media [DMEM and HAM's F12 (1:1) (Fisher #SH20361), 10% fetal bovine serum, 100 U/ml penicillin and 100 µg/ml streptomycin] at 37 C, 5% CO_2 and passaged every 48h using 0.25% trypsin/0.1% EDTA in a 1:10 dilution. HT-22 cells were plated at 80,000 cells/mL in two 6-well plates (2 mL each well), and grown in full growth media at 37 C, 5% CO_2 for 24 h to 60% confluency, then differentiated with neurobasal for 24 h. After differentiation, the plates were treated with lithium isotopes in the form of lithium carbonate for 24h. The ^{6}Li-dominant isotope contained 95% ^{6}Li and 5% ^{7}Li. The ^{7}Li-dominant isotope contained 92% ^{7}Li and 8% ^{6}Li. The isotope formulations are referred to by their dominant isotope for simplicity. Plate #1 was treated as: control in duplicate, 4 mM ^{6}Li in duplicate, 4 mM ^{7}Li in duplicate. Plate #2 was treated as: control in duplicate, 4 mM, ^{6}Li, 4 mM ^{7}Li, 8 mM ^{6}Li, 8 mM ^{7}Li. Plate #1 was harvested using the trypsin technique and plate #2 was harvested using the lysis buffer technique. For each treatment group, the media and the cell lysate were obtained and stored at -20 C until taken to the ICP-MS for analysis.

10 cm^2 Plates

HT-22 cells were cultured in full growth media and then plated at 80,000 cells/mL in three 10cm^2 plates (10 mL each), and grown in full growth media at 37C, 5% CO_2 for 24 h to 60% confluency, then differentiated with neurobasal for 24 h. After differentiation, one plate was left as control, one plate was treated with 4 mM ^{6}Li and one treated with 4 mM ^{7}Li for 24 h. The cells were harvested using the trypsin technique. For each treatment group the media, the PBS wash, and the cell homogenate were obtained and stored at -20 C until taken to the ICP-MS for analysis.

Through this treatment scheme, ^{6}Li-treated and ^{7}Li-treated cells were grown in two different plates and harvested with two different techniques to allow for comparison.

Before analyzation, all samples were digested in H_2O_2-HNO_3 to destroy organics, then diluted in 2% HNO_3. The digestion, dilution, and analyzation of the samples was kindly carried out by Dr. Brian Kendall, Dr. Chris Yakymchuk, and Sarah McChaugherty to produce dilution-corrected ^{6}Li and ^{7}Li concentrations [ng/ml] as well as the percent content of ^{6}Li and ^{7}Li in each sample (Appendix A), summarized in the following tables 2-1, 2-2, and 2-3.

2.3 Results

Results of 10cm^2 Plates

Treatment Group	Media (ng/mL)		PBS Wash (ng/mL)		Cell Lysate (ng/mL)	
	^{6}Li	^{7}Li	^{6}Li	^{7}Li	^{6}Li	^{7}Li
Control	2.8	5.6	-	-	4.7	9.1
^{6}Li 4mM	21466	1123	1175	66	128	129
^{7}Li 4mM	1660	22846	27	434	73	294

Table 2-1: 10cm^2 Plates Harvested with Trypsin. Table 2-1 illustrates the lithium isotope content in the fractions taken from 10cm^2 plates harvested by trypsin. Each treatment group represents a separate 10cm^2 plate. Thus, one control plate, one plate treated with ^{6}Li at 4mM, and one plate treated at ^{7}Li at 4mM. After 24h of treatment, a sample of the media, a sample of the PBS wash, and a sample of the cell lysate was obtained and analyzed for lithium isotope content by ICP-MS.

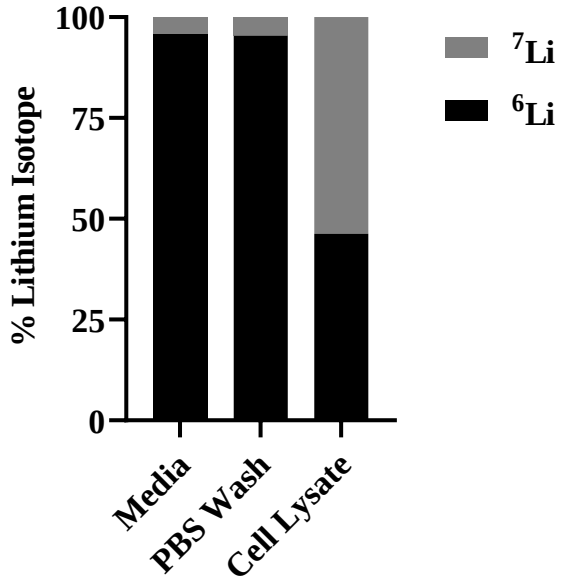

Figure 2-2: Lithium Isotope Content in HT22 Cells Grown in a 10cm^2 Plate Treated with 4mM ^{6}Li for 24 h. *Figure 2-2 illustrates the fraction of ^{6}Li/^{7}Li in each sample. These cells were treated with 4mM ^{6}Li for 24 h and harvested with trypsin. Corresponding to data presented in table 2-1.*

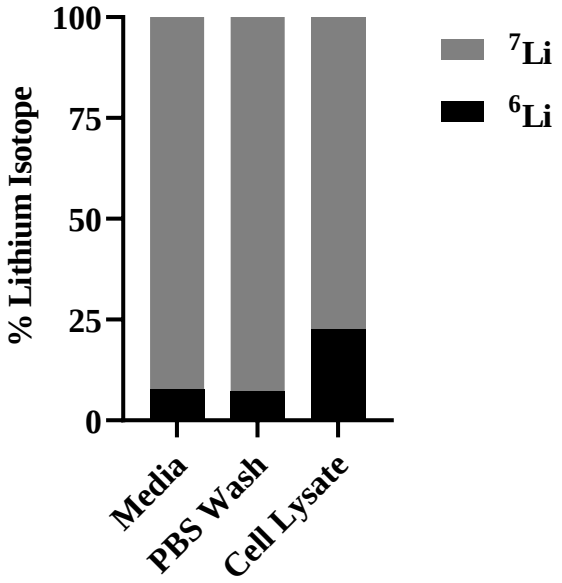

Figure 2-3: Lithium Isotope Content in HT22 Cells Grown in a 10cm^2 Plate Treated with 4mM ^{7}Li for 24 h. *Figure 2-3 illustrates the fraction of ^{6}Li/^{7}Li in each sample. These cells were treated with 4mM ^{7}Li for 24 h and harvested with trypsin. Corresponding to data presented in table 2-1.*

Results of 6-Well Plate #1

Treatment Group	Media (ng/mL)		Cell Lysate (ng/mL)	
	^{6}Li	^{7}Li	^{6}Li	^{7}Li
Control (1)	2.7	7.4	2.6	8.8
Control (2)	51.7	64	2.9	7.7
^{6}Li 4mM (1)	23946	1300	77	12
^{6}Li 4mM (2)	22459	1264	93.2	27
^{7}Li 4mM (1)	1751	23954	8.8	86
^{7}Li 4mM (2)	2775	37684	23.9	140

Table 2-2: 6-Well Plate #1 Harvested with Trypsin. *Table 2-2 illustrates the lithium content in the fractions taken from each well of a 6-well plate harvested by trypsin. Each treatment group represents a separate well. The lithium isotope content in duplicate samples of each treatment group: Control, ^{6}Li 4mM-treated, and ^{7}Li 4mM-treated are presented.*

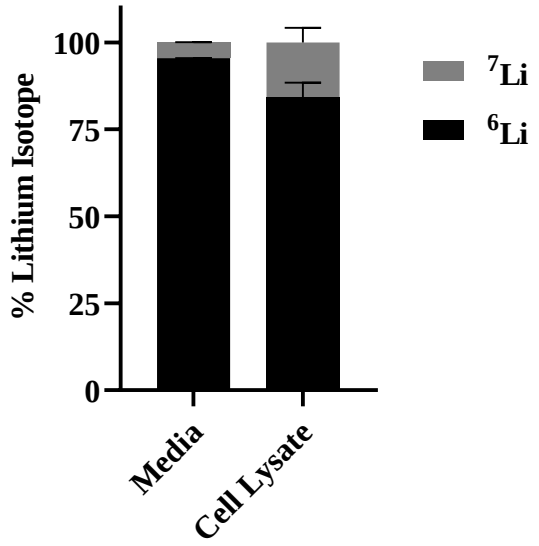

Figure 2-3: Lithium Content in HT22 Cells Grown in 6-Well Plates and Treated with 4mM ^{6}Li for 24 h. *Figure 2-4 illustrates the fraction of ^{6}Li/^{7}Li in each sample. Duplicates [(1) and (2) from table 2-2] were expressed as mean + SEM. These cells were treated with 4mM ^{6}Li for 24 h and harvested with trypsin.*

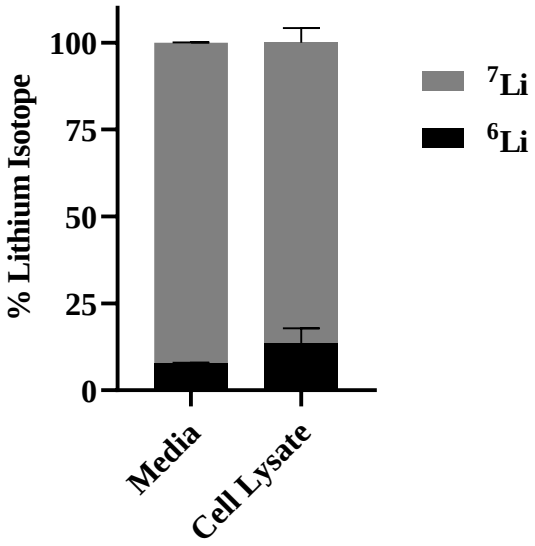

***Figure 2-2*: Lithium Content in HT22 Cells Grown in 6-Well Plates and Treated with 4mM ^{7}Li for 24 h.** *Figure 2-5 illustrates the fraction of ^{6}Li/^{7}Li in each sample. Duplicates [(1) and (2) from table 2-2] were expressed as mean + SEM. These cells were treated with 4mM ^{7}Li for 24 h and harvested with trypsin.*

Results of 6-Well Plate #2

Treatment Group	Media (ng/mL)		Cell Lysate (ng/mL)		Cell Protein (ug/uL)
	^{6}Li	^{7}Li	^{6}Li	^{7}Li	-
Control 1	3.0	6.6	1.4	4.3	-
Control 2	3.4	28	1.5	3.9	-
^{6}Li 4mM	25788	1408	62	8.6	1.739
^{6}Li 8mM	39415	2426	133	41	2.006
^{7}Li 4mM	1608	21916	16	49	2.078
^{7}Li 8mM	3451	46871	26	116	1.561

***Table 2-3: 6-well plate #2 Harvested with Lysis Buffer**. Table 2-3 illustrates the lithium content in the fractions taken from the 6-well plate harvested by lysis buffer in addition to the correlating cell protein concentration. Each treatment group represents a separate well. Thus, the lithium isotope content in samples of each treatment group: Control, ^{6}Li 4mM-treated, ^{7}Li 4mM-treated, ^{6}Li 8mM-treated, and ^{7}Li 8mM-treated are presented.*

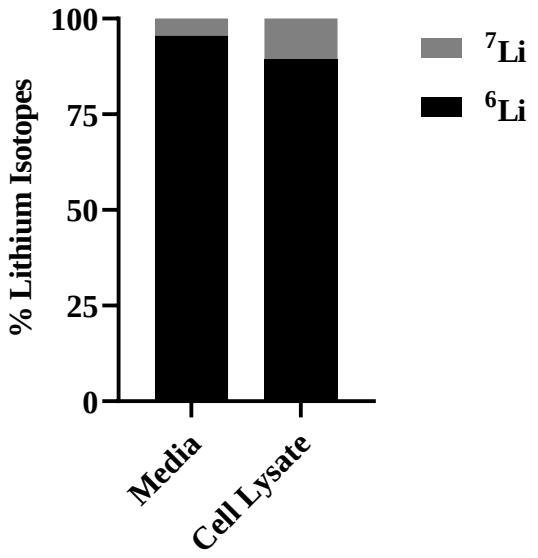

***Figure 2-6: Lithium Content in HT22 Cells Grown in 6-Well Plates and Treated with 4mM ^{6}Li for 24 h.** Figure 2-6 illustrates the fraction of ^{6}Li/^{7}Li in each sample. These cells were treated with 4 mM ^{6}Li for 24 h and harvested with lysis buffer. Corresponding to data presented in table 2-3.*

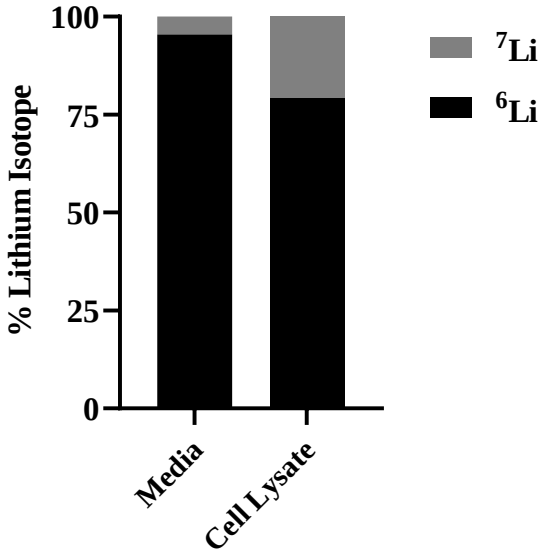

***Figure 2-7: Lithium Content in HT22 Cells Grown in 6-Well Plates and Treated with 8mM ^{6}Li for 24 h.** Figure 2-7 illustrates the fraction of ^{6}Li/^{7}Li in each sample. These cells were treated with 8 mM ^{6}Li for 24 h and harvested with lysis buffer. Corresponding to data presented in table 2-3.*

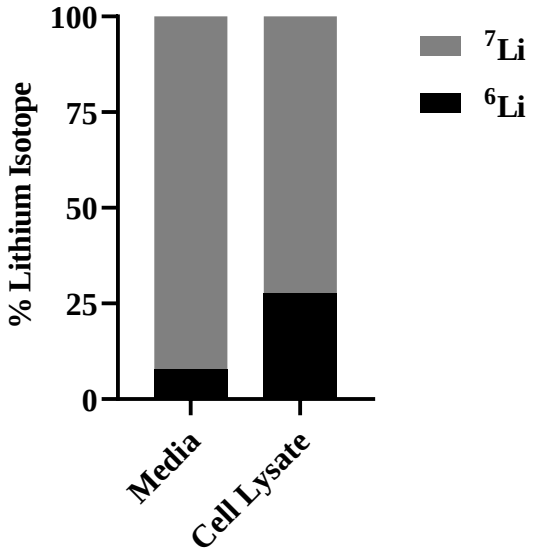

Figure 2-8: Lithium Content in HT22 Cells Grown in 6-Well Plates and Treated with 4mM ^{7}Li for 24 h. *Figure 2-8 illustrates the fraction of ^{6}Li/^{7}Li in each sample. These cells were treated with 4 mM ^{7}Li for 24 h and harvested with lysis buffer. Corresponding to data presented in table 2-3.*

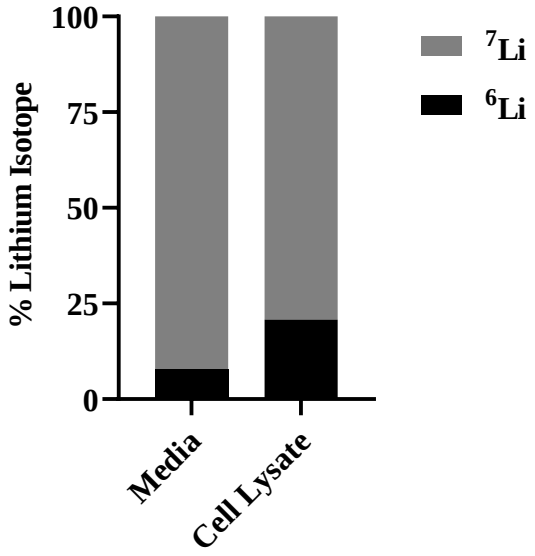

Figure 2-9: Lithium Content in HT22 Cells Grown in 6-Well Plates and Treated with 8mM ^{7}Li for 24 h. *Figure 2-9 illustrates the fraction of ^{6}Li/^{7}Li in each sample. These cells were treated with 8 mM ^{7}Li for 24 h and harvested with lysis buffer. Corresponding to data presented in table 2-3.*

2.4 Results and Discussion

The data allows for quite a few interesting conclusions to be drawn but many more questions arise. The main purpose for this experiment was to develop techniques that would allow quantification of intracellular lithium isotope content, and it seems that this goal was achieved. However, preliminary data comparing intracellular and extracellular lithium isotope ratio is mildly perplexing and warrants closer examination.

The total concentration of lithium in the samples is well within the range of ICP-MS detection threshold in both sizes of plates (6-well and 10 cm^2 plates). Therefore, in future experiments, 6-well plates will exclusively be used as they are more cost-effective and efficient.

The detection limit for ^{6}Li concentrations is 2.6 ng/mL, and the detection limit for ^{7}Li concentrations is 0.17 ng/mL (only applicable before dilution correction, columns C and E in Appendix A). The data is also only semi-quantitative ranging from 2.6 ng/mL to 15 ng/mL for ^{6}Li, and semi-quantitative ranging from 0.17 ng/mL to 1 ng/mL for ^{7}Li (Appendix A). Fortunately, only the control group cell lysates are within the semi-quantitative ranges with the exception of one treatment group: the 8mM ^{7}Li-treated cells. The fact that this sample approached these detection limits is not due to a limit of the actual ICP-MS detection, but due to a high dilution factor. Now that the relative magnitude of lithium concentration in cell lysates is known, future samples can easily be diluted to ensure lithium concentrations are in the proper range for the ICP-MS detection. The control lithium concentrations are within the semi-quantitative range. As of now, it is unknown whether the lithium isotope content detected in the control groups is a valid amount of lithium present in the media, or whether the values are simply error inherent in the ICP-MS. In the future, the control samples can be diluted a lesser amount to answer this question.

Cell Harvest Technique

The technique of cell harvest was a critical aspect to be considered. Trypsinization results in the whole cell being included in the cell lysate, while lysis buffer and centrifugation results in most of the plasma membrane being removed. A significant amount of lithium isotope binding to the cell membrane after PBS wash seems unlikely, but in this research the lysis buffer technique may be more appropriate, as only intracellular lithium isotope content is of interest. The lysis buffer technique is advantageous in that it allows for control of cell count by analyzation of cell protein concentrations. The lysis buffer technique is also appropriate for western blotting

analysis, allowing for the same sample to be analyzed by western blotting and by ICP-MS. This will be quite advantageous for data correlation in future experiments.

The BCA protein assay is often used to quantify cell protein in a homogenate for accurate loading in western blot gels. In this application, it can serve as a control for cell count. The total amount of intracellular space is unknown and variable, and whether the lithium content detected is truly only intracellular is also unknown. But logically it is expected that the intracellular volume scales with cell count and so the total amount of intracellular lithium must also scale with cell count. In this experiment, the BCA assays were performed simply to provide some semblance of preliminary information about the relative cell count in each sample. In the future, it would be better to quantify the protein concentration in each sample then detect whether the resultant lithium concentrations correlate with the protein concentrations. If the lithium concentrations correlate with cell protein, then the assumption that this lysis buffer technique is truly and accurately examining the intracellular concentration of lithium can be trusted slightly more. As of now there is no correlation between the lithium concentration in the sample and protein concentration and the number of replicates is far too low for definitive conclusions to be drawn (table 2-3).

Lithium Isotope Ratios

Between treatment groups, the total amount of lithium detected in the cell lysates was relatively consistent and significantly above control values (tables 2-1 to 2-3). The ratios of intracellular lithium isotopes compared to the ratios of extracellular isotopes are the only perplexing aspect of the data collected. The extracellular media in every sample (tables 2-1 to 2-3) contained the expected ratios of ^{6}Li to ^{7}Li with extremely low variance, indicating the ICP-MS

is certainly capable of detecting isotope concentrations. In figures 2-2 and 2-3, the intracellular lithium isotope content ratio in $10cm^2$ plates harvested with trypsin indicates an enrichment of the least abundant ratio when compared to the media and PBS wash. In figures 2-4 and 2-5, the intracellular lithium isotope content also indicates an enrichment of the least abundant isotope in 6-well plates harvested with trypsin. In figures 2-6 to 2-9, 6-well plates treated with 4 mM and 8 mM of lithium harvested with lysis buffer also show an intracellular enrichment of the least abundant isotope. Due to the constant updates and refinement of the methods, it was not possible to perform a statistical analysis as there were no exact replicates (other than an N = 2 for 6-well plates harvested with trypsin). However, we did observe a consistent enrichment of the less abundant isotope in the cell lysate fraction compared to the extracellular media and PBS wash. What could be responsible for enrichment of the less abundant isotope intracellularly regardless of the extracellular isotope ratio seen in Figures 5-2 to 5-9? The first answer that usually comes to mind – that there is an issue with detection, seems unlikely since the treatment groups contain significantly more total lithium than the negative control groups (the signal is on average 10x greater than the negative controls, and well within the detection limits). So the ICP-MS must be detecting the lithium and not other similar *m/z* ratios in the cellular milieu. The next possible answer is that the plate itself is differentially binding and retaining lithium isotopes, but the PBS wash in the $10cm^2$ plates (table 5-1) shows an isotope ratio identical to the media, albeit with limited replicates and 10x the concentration found in the cell lysates.

The next possible answer for the unexpected intracellular enrichment of the less concentrated isotope is that there could be a biological mechanism driving this fractionation. It is known that lithium is transported through the cell plasma membrane by the various Na^+ channels and pumps, but whether there are different efficacies for each isotope is the main question. The

consistent enrichment of the less concentrated isotopes could suggest that there is a definite steady state dynamic equilibrium of the isotopes closer to 50/50 intracellularly, and the cells are trying to reach that state regardless of the isotopic ratio in the extracellular media. These hypotheses will need to be answered in future experimental designs.

Future Improvements in Data Correlation and Experimental Design

It is important to remember that the lithium detected in the cell lysates only partially (though perhaps mostly) consists of the intracellular lithium content. While every effort to remove the extracellular lithium was made (washing the 6-well plates 2x with 2mL of PBS before harvest), the true ratio of intracellular vs. extracellular lithium in the cell lysate is unknown. To remedy this, future experiments should track the lithium content in multiple PBS washes for each well – this was not done in this experiment for any plates except for the $10cm^2$ plates for reasons of throughput and time limits. Tracking the lithium isotope concentration and ratio in progressive numbers of PBS washes and tracking whether the lithium content in the cell lysate correlates with BCA protein assay results could both serve to help confirm how quantitatively these methods examine the intracellular content.

Data correlation will no doubt help in determining the validity of the methods, but to shed more light on the biological mechanisms involved, more experimental conditions should be explored. Differing time points and lithium isotope composition would be extremely valuable in determining whether there truly is a dynamic equilibrium of isotope fractionation across the membrane. Variable time points could be used to track the isotopic ratio changes, and variable isotope compositions in the media may change the intracellular equilibrium of isotopes.

2.5 Conclusion

Overall, this first step into ICP-MS analyzation of cellular fractions has been a success. The optimum techniques to minimize effort and investment have been identified, and it has been proven that the ICP-MS can detect the lithium concentrations present in the cellular fractions. However, the perplexing data showing intracellular enrichment of the less concentrated isotope is still a question with no satisfying answer. Further research with a greater number of testing conditions and more correlation between data sets should allow the determination of exactly whether the HT22 plasma membrane is differentially fractionating the two lithium isotopes.

Chapter 3 : Lithium Isotope Toxicity on HT22 Cells

3.1 Objectives and Hypotheses

There has been no identified research done on the toxicity of lithium in cell lines to determine whether there is a reproducible isotopic effect. The previously mentioned research on the LD50 of the isotopes in rats and the ^{6}Li LD50 was found to be 13meq/kg while the LD50 of ^{7}Li was 16meq/kg[138] but this finding is controversial[137]. However, our hypothesis remains that the two lithium isotopes would present differential toxicity rates on HT22 cells

(Note: A second hypothesis was generated while carrying out these experiments: perhaps neurobasal media is causing L-cystine and NMDA-mediated excitotoxicity, confounding the results of the lithium isotope assays[165]. To test this hypothesis, a second set of experiments was designed to compare the effects of lithium isotopes on both neurobasal media and DMEM-treated cells.)

3.2 Materials and Methods - MTT Toxicity Assays

Cell viability studies are often used in early preclinical drug trials to provide insight on how toxic a drug is to living cells. The dimethylthiazol diphenyltetrazolium (MTT) bromide assay is advantageous because it allows quick measurement of a proxy for cell viability[169]. The principle of the MTT assay is based on the use of colourimetry to gauge cell metabolism. MTT, a yellow salt with peak light absorbance of around 690nm, is metabolized by living cells to formazan, a purple salt with peak absorbance of around 570nm[169]. This drastic colour change can be quantified using absorbance spectroscopy to give an indication of how many cells are alive after drug treatment still able to metabolize the MTT.

In this research, MTT assays were used to determine if the lithium isotopes had any measurable difference in toxicity. The ^{6}Li-dominant isotope contained 95% ^{6}Li and 5% ^{7}Li. The ^{7}Li-dominant isotope contained 92% ^{7}Li and 8% ^{6}Li. The isotope formulations are referred to by their dominant isotope for simplicity. The dependant variable being cell metabolic rate (an indication of cell viability), and the independent variable being lithium isotope concentration.

HT22 cells were cultured in full growth media [DMEM and HAM's F12 (1:1) (Fisher #SH20361), 10% fetal bovine serum, 100 U/ml penicillin and 100 µg/ml streptomycin] at 37 C, 5% CO_2 and passaged every 48h using 0.25% trypsin/0.1% EDTA in a 1:10 dilution. For experimentation, the cells were plated at 8,000 cells/well in a 96-well plate and grown in full growth media for 24h to 60% confluency. The cells were then differentiated with neurobasal media containing 5 mM N2 supplement and 5 mM L-glutamine for 24h. After differentiation, the cells were treated with both lithium isotopes at concentrations ranging from 8mM to 32mM for 24h using sterile-filtered MilliQ water as a vehicle at 0.2M. After this, the media was changed to phenol-free DMEM/F12 (1:1) with 10% MTT solution. The cells were incubated for 2.5h at 37C to metabolize the MTT. The cells and formazan crystals were then solubilized with a solution of 90% IPA, 10% Triton X-100, and 0.1M HCl and the absorbance of each well at 570nm and 690nm was determined by spectroscopy. The 690nm signal was subtracted from the 570nm signal to control for unmetabolized MTT. All treatment groups were normalized to the true control and expressed as a ratio of survivability to produce Figure 3-1.

In an effort to provide more data on the question of whether neurobasal is causing excitotoxic effects (and whether lithium is rescuing those effects), more 96-well plates were seeded at 8,000 cells/well and grown for 24h to 60% confluency. The media in half of the wells was changed to just DMEM [DMEM and HAM's F12 (1:1) (Fisher #SH20361] and the other half

of the wells were changed to neurobasal media. The cells were then immediately treated with lithium isotopes for 24h. After treatment, the cells were incubated with MTT, solubilized, their absorbency was read, and the data was analyzed exactly as previously described to produce Figure 3-2.

3.3 Results

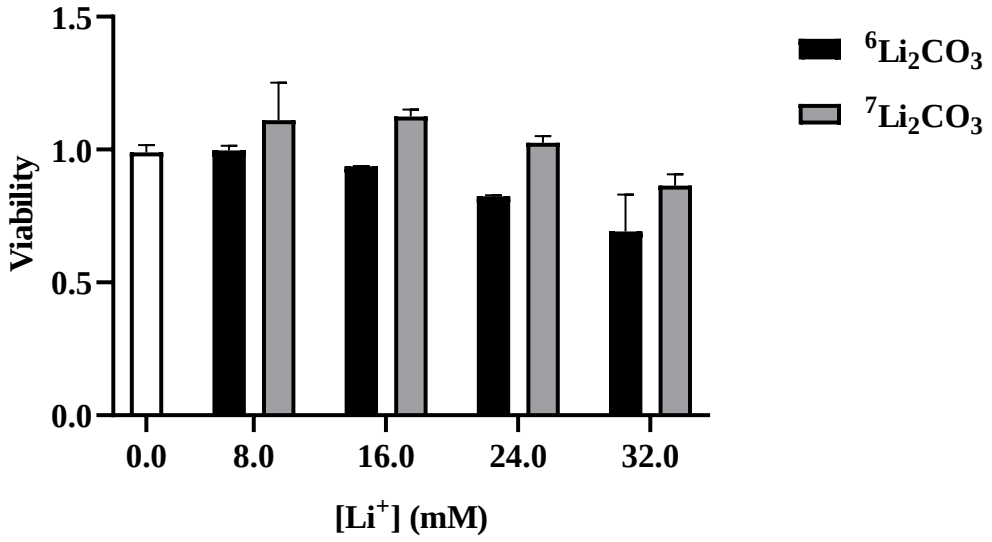

Figure 3-1: HT22 Viability as a Result of Lithium Isotope Treatment in Neurobasal Media: *Data from two replicates (N=2) are presented as mean + standard error of the mean (SEM). No statistical analysis has been performed due to the low number of replicates.*

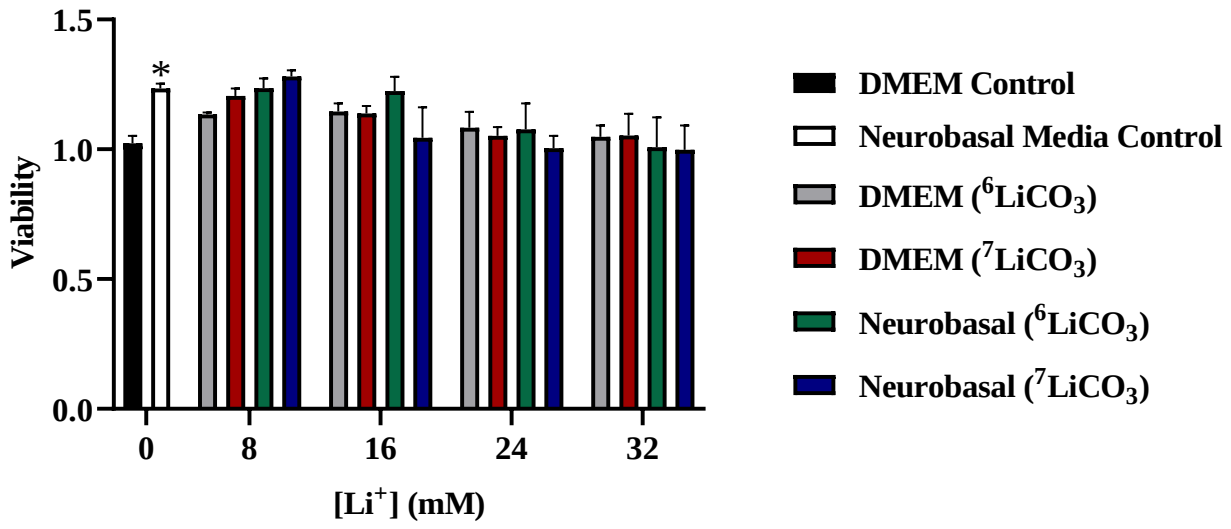

Figure 3-2: HT22 Viability as a Result of Lithium Isotope Treatment in DMEM and Neurobasal Media. *Data presented as mean + SEM. (N=3, two-way analysis of variance (ANOVA), * = p <0.05). Data represents the simultaneous comparison of HT22 cell viability when treated with lithium isotopes in DMEM and Neurobasal media. A significant difference was found between control DMEM and neurobasal media-treated cells.*

3.4 Discussion

Figure 3-1: HT22 Viability as a Result of Li^+ Isotope Treatment

The results reported in figure 3-1 are representative of two independent replicates. However, the finding that $^7LiCO_3$ (natural lithium) does not seem to cause marked toxicity even at high concentrations is not consistent with the literature. Literature values of lithium toxicity indicate an approximate 20% kill rate at 10mM[170]. There is some evidence to indicate that neurobasal could have excitotoxic effects[165], and the neuroprotective effects of lithium are well documented. This was initially hypothesized to be the reason why there is such a drastic increase in cell viability even at high lithium concentrations – conflicting effects by neurobasal and lithium. However, further research into cell viability as a result of (only) DMEM and neurobasal media treatment seems to not support this hypothesis as shown in figure 3-2.

Figure 3-2: HT22 Viability as a Result of Li^+ Isotope Treatment in DMEM and Neurobasal Media

Figure 3-2 represents data harvested from three 96-well plates. Each plate was treated in such a way to compare both DMEM and neurobasal-treated cells for each concentration of lithium. This was intended to give an indication as to whether neurobasal could be causing undue amounts of excitotoxicity in lithium concentrations ranging from 0-32 mM.

The comparison of the two control columns indicate that there is no excitotoxicity caused by neurobasal media compared to DMEM. In fact, lithium-free neurobasal has significantly greater cell viability than just lithium-free DMEM – exactly as expected if neurobasal is not causing excitotoxicity. Interestingly, as the lithium concentration increases, there is still no significant lithium toxicity seen in either the DMEM or neurobasal-treated groups. The possible toxic effect of ^{6}Li observed in Figure 3-1 has not been replicated in either DMEM or neurobasal-treated groups. This could mean that the possible differential toxicity seen in Figure 3-1 is mediated through mature-neuronal attributes that are only achieved after sufficient time (48h or more) in neurobasal.

3.5 Conclusions

In these cell viability assays, it seems that lithium toxicity is not straightforward and determination of lithium toxicity on HT22 cells is proving to be difficult. This could indicate that the neurobasal media model is introducing uncontrolled-for variables, or it could indicate that these HT22 cells are especially resistant to the toxic effects of lithium. Future experiments at multiple time points of lithium treatment and neurobasal differentiation would shed light on the extremely complex effects of lithium on HT22 cells.

Chapter 4 : Lithium Isotope Inhibition of GSK-3-β Kinase Activity

4.1 Objectives and Hypothesis

As mentioned, previous experiments indicate that ^{6}Li is more toxic in rats and is held at a higher concentration in the neuronal cell and the red blood cell than ^{7}Li, but to no known replications have been reported. The leading hypothesis for how Li^{+} directly inhibits GSK-3-β is that Li^{+} competes with Mg^{2+} for specific protein binding sites and in the ATP-Mg complex. Following this logic, since ^{6}Li is less massive than ^{7}Li, and even less massive than Mg^{2+} (the natural and most effective ion for each of these binding sites), it was hypothesized that lithium isotopes would show differential effects on the kinase activity of GSK-3-β.

4.2 Materials and Methods - The ADP-Glo Assay

The ADP-Glo assay by Promega is used to quantify the activity of ADP-producing enzymatic reactions. It is a bioluminescent, universal assay that is compatible with virtually every kinase. A kinase is an enzyme that catalyzes the transfer of a phosphate from ATP to a substrate, producing ADP and a phosphorylated substrate. GSK-3-β is one such ADP-producing kinase that is a major kinase of Tau and many other intracellular proteins involved in neuroprotection and metabolism.

The ADP-Glo assay used in this research was specifically designed for use with GSK-3-β to allow for high-throughput screening of kinase activity as a result of drug treatment. The assay kit included active GSK-3-β and a proprietary substrate derived from glycogen synthase we will call “GSK substrate”. The general layout of the experiment is to react the kinase with its substrate in a kinase buffer with the inhibitor (Li^{+} isotopes) for a length of time, then add the ADP-Glo Reagent to bind and deplete all ATP, then add the kinase detection reagent which both

phosphorylates the remaining ADP (produced by the kinase reaction) into ATP and luminesces using that same ATP[171]. In this way, the kinase activity can be quantified by the relative light produced (in relative light units – RLU) as a result of ADP and kinase detection reagent binding.

All kinase reactions were performed in Reaction Buffer A (40 mM Tris, pH 7.5, 20 mM $MgCl_2$, and 0.1 mg/mL BSA) at room temperature in 5 uL total volume in a 384-well, round bottomed, white plate as directed by Promega.

The ADP-Glo kit included all reagents required to carry out the experiment except for the kinase reaction buffer A (made in lab with on-hand reagents from Sigma Aldrich using manuals from Promega). The GSK-3-β was diluted in kinase reaction buffer A to a concentration of 2ng/uL. The GSK substrate was diluted to 0.2ug/uL with 125uM ATP. The lithium isotopes in the form of lithium carbonate were obtained from Sigma Aldrich. The ^{6}Li-dominant isotope contained 95% ^{6}Li and 5% ^{7}Li. The ^{7}Li-dominant isotope contained 92% ^{7}Li and 8% ^{6}Li. The isotope formulations are referred to by their dominant isotope for simplicity. The lithium isotopes ^{6}Li and ^{7}Li were each diluted to 1.25mM, 2.5mM, 5mM, 10mM, 20mM, 40mM, 80mM in kinase reaction buffer A and the pH was adjusted as needed to 7.5.

Each well of the 384-well plate contained 5uL total. First 1uL of ^{6}Li or ^{7}Li dilution was added to each well, then 2uL of GSK-3-β dilution, then 2uL of GSK substrate dilution with 125uM ATP. In the control wells, the 1uL was simply devoid of Li^+. After 1h of reaction time at room temperature, the reaction was stopped by addition of 5uL of ADP-Glo reagent to each well and left to incubate at room temperature for 40min. After incubation, 10uL of kinase ketection reagent was added and after 30min, a microplate reader was used to measure the resulting luminescence. The luminescence in each well as measured by relative light units (RLU) was expressed as a ratio of the control group luminescence. Thus, relative luminescence values were

obtained detailing the direct inhibition of GSK-3-β activity by both lithium isotopes at concentrations of 0.25mM. 0.5mM, 1mM, 2mM, 4mM, 8mM, and 16mM.

4.3 Results

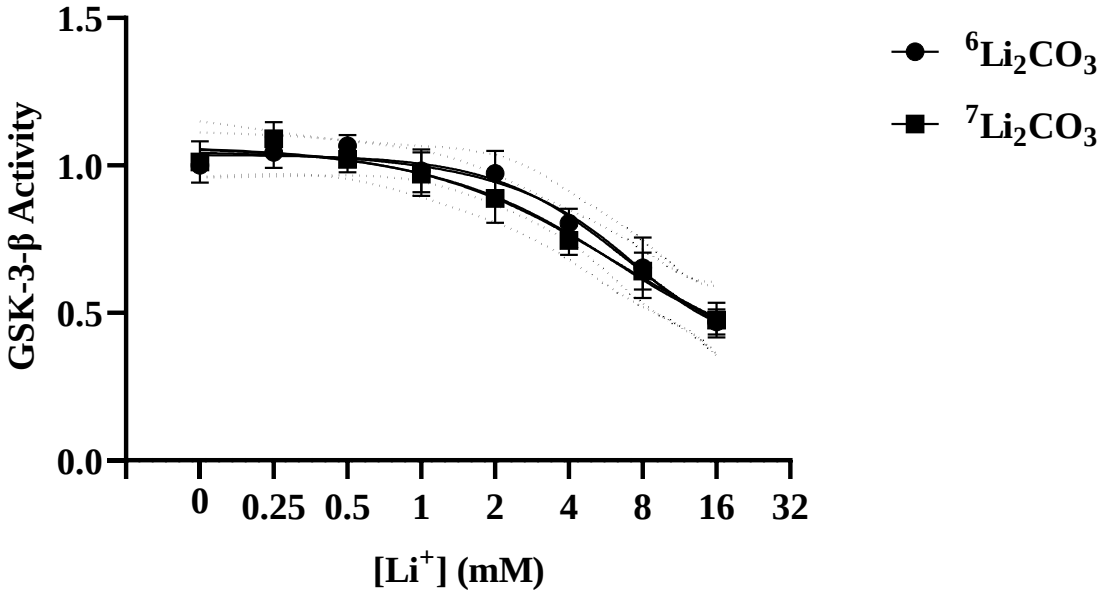

Figure 4-1: Direct Inhibition of GSK-3-β by Lithium Isotopes*. Data represents the mean + standard error of the mean (SEM) of 5 replicates (N=5). The X-axis indicates molarity of the Li^+ ion, not the molarity of Li_2CO_3. The data was fitted to a sigmoidal dose-response curve and the ^6Li R^2 = 0.7190 and the ^7Li R^2 = 0.7052. The half maximal inhibition (IC50) for the ^6Li curve was calculated to be 6.883 mM and the IC50 for the ^7Li curve was calculated to be 6.342 mM. The dotted lines surrounding the curves are the 95% confidence intervals.*

4.4 Discussion

The results presented in figure 4-1 do not indicate a significant difference between the effects of isotopes on GSK-3-β activity at any concentration, and the calculated half-maximal inhibition concentrations (IC50s) of 6.883 mM for ^6Li and 6.342 mM for ^7Li are not significantly different.

The curve obtained seems to generally correlate with literature values on lithium inhibition of GSK-3-β with a couple caveats. This experiment was designed simply to determine

if there is a difference in GSK-3-β activity as a result of lithium isotope treatment. There were no tests done at extremely high lithium concentrations because of limitations due to experimental design and due to determination that there was no need for further testing based on the extremely similar values at these lower concentrations. The lithium isotope salts used in all experiments were Li_2CO_3 in an attempt to correlate with previous findings in the literature and by Dr. Mielke and Yuyi Xu at the University of Waterloo. Li_2CO_3 is not very soluble, with its solubility topping out at around 200 mM in deionized water, and much lower in salt-enriched kinase buffer. Thus, the maximal concentration consistently achieved in kinase buffer was 80 mM, resulting in 16 mM final lithium isotope concentration.

The calculated IC50s are valid only for comparison differences between the isotopes in this particular experiment. Analysis of the curve indicates that significant inhibition of GSK-3-β activity only begins at around 2-4 mM while the half maximal inhibition concentrations (IC50s) are at 6.883 and 6.342 mM. These IC50s are higher than expected when compared with the literature[172], but are explained by the concentrations of Mg^{2+} used in the assay. Because the Li^+ inhibition of GSK-3-β is dependant on the concentration of free Mg^{2+}, an increased amount of Mg^{2+} will result a decreased inhibitory effect of Li^+ [173]. The total amount of Mg in most animal cells is estimated to be approximately 17-20 mM with approximately 5 mM bound to cytosolic ATP, phosphonucleotides in general, and phosphometabolites[174]. Free Mg^{2+} is estimated to be between 0.5-1 mM[175]. As such, the local Mg^{2+} concentrations are vital to the effect of lithium on enzyme activity both *in-vitro* and *in-vivo*.

In the future, if further testing is deemed needed, perhaps it would be worthwhile to adapt these methods or find a different kinase activity test that would allow the use of a lower amount

of Mg^{2+} that would better approximate the estimated intracellular physiological levels of Mg^{2+} at around 0.5 – 5 mM.

4.5 Conclusions

The results indicate that there is no significant difference between Li^{+} isotope inhibition of GSK-3-β activity for these experimental conditions. The similar calculated IC50s, low error rate, and extremely similar means between the isotopes for each concentration indicate that there is likely no significant difference, but repetition of this experiment using physiological concentrations of Mg^{2+} may be more relevant. As it stands, using the recommended conditions of the Promega GSK-3-β activity assay, there is no difference evident between the lithium isotope inhibition of GSK-3-β.

Chapter 5 : Lithium Effects on GSK-3-β Phosphorylation in HT22 Cells

5.1 Objectives and Hypothesis

The question of whether lithium isotopes have a differential effect on the phosphorylation of GSK-3-β on serine 9 (S9) is one borne out of the understanding that S9 phosphorylation will inhibit GSK-3-β activity[77]. Lithium is known to inhibit GSK-3-β directly through Li^{+}-Mg^{2+} competition and indirectly by increasing S9 phosphorylation[24,25,80]. Based on the limited literature regarding isotopic differences, it was hypothesized that there would be a differential S9 phosphorylation rate according to treatment by lithium isotopes.

5.2 Materials and Methods - The Western Blot

The western blot is a well-established technique used to detect proteins in a sample of cell or tissue homogenate using gel electrophoresis and protein-specific antibodies. The following procedures were completed to examine the effect of lithium isotopes on the phosphorylation of the GSK-3-β S9 site in HT22 cells.

HT22 cells were cultured in full growth media [DMEM and HAM's F12 (1:1) (Fisher #SH20361), 10% fetal bovine serum, 100 U/ml penicillin and 100 μg/ml streptomycin] at 37 C, 5% CO_2 and passaged every 48h using 0.25% trypsin/0.1% EDTA in a 1:10 dilution. These cells were then plated at 8,000 cells/well in a 6 well plate and grown in full growth media at 37C, 5% CO2 for 24h to 60% confluency, then differentiated with neurobasal for 24h. After differentiation, the wells were labelled into six treatment groups: control 1, control 2, 4mM ^{6}Li, 4mM ^{7}Li, 8mM ^{6}Li, and 8mM ^{7}Li. The ^{6}Li-dominant isotope contained 95% ^{6}Li and 5% ^{7}Li. The ^{7}Li-dominant isotope contained 92% ^{7}Li and 8% ^{6}Li. The isotope formulations are referred to by their dominant isotope for simplicity. These treatment groups were designed to test whether there

is a difference in the phosphorylation of serine 9 of GSK-3-β after treatment with lithium isotopes.

Cell Harvest

After 24h of treatment with lithium isotopes, the cells were ready for harvest. The media was aspirated off and the wells were washed with 3mL ice cold PBS. 70uL of lysis buffer [20 mM Tris-HCl pH 7.5,150 mM NaCl, 1 mM EDTA, 1 mM EGTA, 30 mM sodium pyrophosphate,1 mM betaglycerophosphate, 1 mM sodium orthovanadate (Na3VO4), 1% triton and 1% Halt Protease and phosphatase inhibitor (Thermo)] was added to each well. The cells were scraped off the well and the lysates were homogenized using fine-gauge syringes then centrifuged at 14,000g for 20min at 4C. The supernatants were collected and frozen at -20C until further use.

SDS-PAGE

8% polyacrylamide gels 1.5mm thick were made and stored until needed in a 4 C refrigerator. The total protein content in each homogenate was determined using a BCA protein assay to allow for precise aliquoting to each lane of the polyacrylamide gel. The protein was then added to 3x loading buffer [240 mM Tris-HCl at pH 6.8, 6% w/v SDS, 30% v/v glycerol, 2% w/v bromophenol blue, 2% v/v 50 mM DTT, and 5% v/v β-mercaptoethanol] then heated to 95°C for 5 min. This linearizes and imparts a net negative charge to the proteins to ensure that their movement through the polyacrylamide gel is proportional to their molecular weight. 15ug of protein was accurately loaded to each well in the gel along with a ladder to provide a standard to compare molecular weights. An electric current was passed through the gel at 125 V for

approximately 1.5 h and, since each protein was given a net negative charge by the SDS, the protein migrated towards the positive terminal. This resulted in a gel containing protein separated out spatially by molecular weight, where the smaller proteins were less restricted and travelled further than the larger proteins.

Wet Electrophoretic Transfer

To detect the protein, it was transferred from the polyacrylamide gel to a PVDF membrane able to bind it. These transfers were completed using the Towbin method[176]. The gel was first allowed to equilibrate in transfer buffer [25 mM Tris base, 190 mM Glycine, 20% methanol, and 80% MilliQ water] for 15 min then sandwiched against the PVDF membrane between positive and negative terminals. Running electricity through the layers for 16 h at 50 amps at 4 C caused the protein to migrate from the gel to the membrane. After completion, the membranes were stained with ponceau dye to allow visualization of the protein and confirmation that the transfer completed correctly. The ponceau was removed by 5 min of 0.1 M NaOH followed by washing with Tris-buffered saline (20 mM Tris base, 150 mM NaCl, pH 7.6) plus 0.1% Tween (TBST) 3x for 10min.

Immunodetection

The membranes were blocked with either 5% w/v BSA or milk (BSA for phosphor-detecting antibodies, non-fat milk for total protein detecting antibodies) in TBST for 1 h at room temperature followed by incubation with primary antibody in blocking buffer overnight at 4C. Membranes were then washed 3x 10min with TBST then incubated with secondary antibody (anti-rabbit) for 1h at room temperature. After another set of 3x 10min washes in TBST, 1.5mL

of chemiluminescent substrate (Luminata Crescendo - Millipore) was added to the membranes and the resultant chemiluminescence was detected with a Kodak 4000MM Pro Imaging Station. After imaging, the membranes were stripped and re-probed with other antibodies. The three analyzed proteins were: totGSK-3-β, pGSK-3-β, and β-actin.

5.3 Results

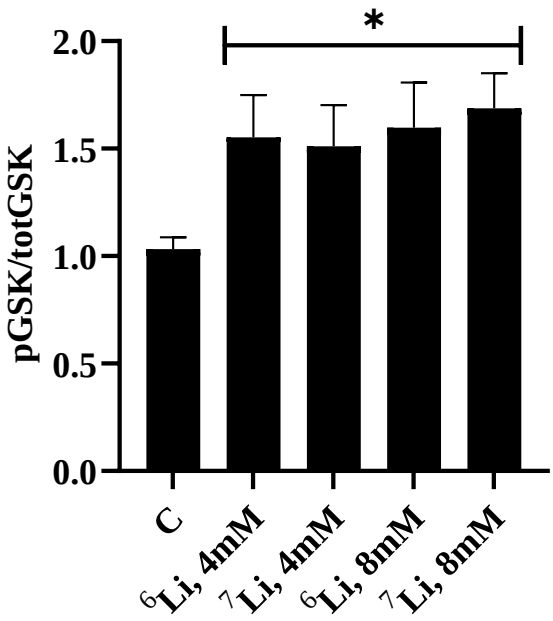

Figure 5-1: GSK-3-β (S9) Phosphorylation as a Result of Li Isotope Treatment. *Figure 5-1 represents data from eight independent 6-well plates (N=8). Data presented as mean + SEM. All signals were normalized by β-actin and total GSK-3-β was not affected by lithium treatment. Welch's unequal variance t-tests were calculated between all treatment groups. No significant differences in phosphorylation of S9 between the lithium isotopes were found, however a significant increase in phosphorylation was found in all lithium-treated groups when each were compared to the control group (C) (* = p<0.05).*

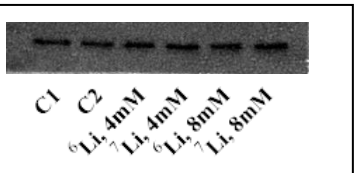

Figure 5-3: totGSK-3-β. *A representative blot of the total GSK-3-β protein as shown in Figure 5-1.*

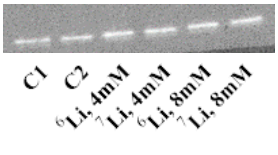

Figure 5-2: pGSK-3-β. *A representative blot of the S9 phosphorylated GSK-3-β protein as shown in Figure 5-1.*

5.4 Discussion

The significant ~1.5-fold increase in phosphorylation between control and all the lithium-treated groups was as expected[177,178,76]. But there is no indication of a significant difference between any of the lithium-treated groups. Thus, the conclusion that lithium isotopes ^{6}Li and ^{7}Li do not result in differential phosphorylation of GSK-3-β at the S9 site is appropriate.

Phosphorylation of the S9 site is well known to result in inhibited GSK-3-β kinase activity. However, this is not the only phosphorylation site that controls the activity of GSK-3-β and the overall activity of GSK-3-β may not be completely described by this site. Phosphorylation of TYR216 can increase GSK-3-β activation. Some research suggests that the overall activity level of GSK-3-β *in vivo* is more accurately correlated with phosphorylation of TYR216 than S9[76]. Since the total activity of GSK-3-β is controlled by more than phosphorylation of S9, characterization of the TYR216 site is a next step to elucidate the true activity level of GSK-3-β in response to lithium isotopes. Perhaps future research on the TYR216 site, when combined with the data presented here, could answer whether the total activity of GSK-3-β is altered differentially by lithium isotopes in the HT22 neuronal cell.

The S9 site on GSK-3-β is phosphorylated by AKT (PKB)[78], PKA[79], Pi-3-K[80], and PKC[81] and is thus only indirectly affected by lithium. Since GSK-3-β S9 is phosphorylated by so many kinases, most of them affected by lithium, a significant difference between the isotopes would be surprising indeed, as it would indicate that every enzyme has the same preference for one isotope over the other. It is likely not the case (even if the isotopic effect exists) that one isotope is more biologically active across all enzymes. The literature indicates that the binding sites of each enzyme are sufficiently variable to either allow Li^{+} to effectively compete with Mg^{2+} or not, which explains how lithium can directly inhibit some enzymes but not others[24]. And if the

variability of different enzyme binding sites is great enough to (seemingly randomly) discriminate between Mg^{2+} and Li^{+}, it is likely that the variability is great enough across all enzymes to not *consistently* discriminate between the lithium isotopes. It could be the case that each enzyme has its own slight preference for each isotope. In that case, examination of such phosphorylation sites by western blot using these methods may never reveal an isotopic effect even if it exists. Perhaps future experiments may be benefited by identification of less-promiscuous phosphorylation sites regulated primarily by one kinase that is directly inhibited by lithium to better track down whether a physiologically relevant isotopic effect exists in the cultured cell or living rat.

5.5 Conclusions

The S9 phosphorylation from lithium treatment in this research corresponds very well to known literature values but no isotopic effect has been found[177]. The lack of isotopic effect on the phosphorylation of S9 could indicate that there is no isotopic effect, or it could indicate the site chosen was regulated by too many kinases for a unidirectional isotopic effect to be detected. The fact that GSK-3-β is regulated by more than one site (S9 and TYR216) also indicates that the true physiological activity of GSK-3-β in response to lithium isotope treatment was likely not captured by this set of data. Future inquiries into phosphorylation states as a result of lithium treatment could be benefited by examining phosphorylation sites that are regulated by few kinases to allow the best possible chance of finding a kinase that is truly differentially inhibited by lithium isotopes *in-vivo* or *in-vitro*.

Chapter 6 : Comments, Conclusions, and Future Directions

The hypothesis that lithium isotopes have differential effects on the neuron, while not especially well supported, is far from impossible. Previous research has either not been replicated or outright challenged the hypothesis as incorrect, but the experiments shown here indicate that the HT22 cells may well be able to fractionate lithium isotopes across the plasma membrane.

The experiments reported in Chapter 2: Lithium Isotope Fractionation by the Neuron Plasma Membrane has resulted in perhaps the most thought-provoking set of data. While the original objectives - to develop sample-harvesting techniques for ICP-MS analysis of HT22 cells - were accomplished, the preliminary data concerning the intracellular isotope ratio has raised a multitude of questions. The consistent intracellular enrichment of the less abundant isotope seems to point to a strong biological mechanism bent on maintaining the intracellular isotope ratio more equally than the ratios the cells were treated with extracellularly. Future investigations would be well-served by experiments designed to track the permeation of lithium isotopes into the cell over multiple timepoints to elucidate more of the dynamic isotope kinetics across the plasma membrane. Treating the cells with a 50/50 ratio of lithium isotopes would also be a good plan, as it would allow rather quick determination of whether a mechanism exists that is enriching one of the isotopes.

The results presented in Chapter 3: Lithium Isotope Toxicity on HT22 Cells do not generally show significant lithium toxicity. Comparison of lithium toxicity on HT22 cells in DMEM and neurobasal media revealed no significant isotope toxicity on undifferentiated HT22 cells and revealed that neurobasal media is not causing excitotoxic effects. However, there seems to be a preliminary difference between the isotopic toxicities in differentiated cells, with ^{6}Li

much more toxic than ^{7}Li. These findings could suggest that the ^{6}Li toxicity is mediated through aspects only expressed in HT22 cells that have been differentiated for 48 h or more. More replicates must be completed before any conclusion can be reached as to whether lithium isotopes have different toxicities on the HT22 cell.

In Chapter 4: Direct Lithium Isotope Inhibition of GSK-3-β Kinase Activity, the possibility that lithium isotopes may differentially compete with Mg^{2+} in the ATP-Mg complex and in the corresponding binding site of GSK-3-β was explored. The supporting literature indicates that the local concentration of Mg^{2+} is of great importance in the determination of GSK-3-β activity inhibition by lithium. The results presented here indicate there simply was no isotopic difference in the inhibition of GSK-3-β. However, it seems that each enzyme itself determines if lithium can interact significantly in the enzyme-ATP-Mg complex, indicating that perhaps differential isotopic inhibition is dependant on the enzyme. There are many other enzymes directly inhibited by Li^{+} such as myo-inositol-1-phospatase and IMPase by non-competitive inhibition[179]. Perhaps it could be justified to test the direct inhibition of lithium isotopes on some of these other enzymes in the future.

The results in Chapter 5: Lithium Effects on GSK-3-β Phosphorylation in HT22 Cells are well corroborated by the existing literature. The treatment of HT22 cells with 4 mM and 8 mM of lithium isotopes resulted in an expected increase in S9 phosphorylation indicating inhibition, but no isotopic difference. Since GSK-3-β is regulated by the TYR219 site as well as the S9 site, the total activity of GSK-3-β was not completely captured by this data. Future experiments investigating phosphorylation of GSK-3-β at the TYR216 site and correlating that with the S9 data presented here would provide a much more complete picture of the effect of lithium isotopes on overall activity of GSK-3-β.

Lithium has long been used to treat patients with bipolar disorder. Recent research indicates it may be effective in the treatment of Alzheimer's disease through reduction of chronic GSK-3-β overactivation and resultant neuronal degradation. These effects seem to be mediated through generally decreasing neuronal excitability but also increasing Wnt and mTOR signalling resulting in an increase in transcription of neuronal-support genes. These findings provide strong motivation for the development of lithium as a treatment for neurodegenerative diseases and for the characterization of lithium isotopic effects on the neuronal cell. While most of these presented data sets do not indicate statistical significance, the data presented here in chapter 2 suggests that lithium isotopes may be differentially transported across the neuronal plasma membrane and provides an avenue for possible improvement in the use of lithium as a medication.

References

1. Turekian, K. K. & Wedepohl, K. H. Distribution of the elements in some major units of the earth's crust. *Bull. Geol. Soc. Am.* (1961) doi:10.1130/0016-7606(1961)72[175:DOTEIS]2.0.CO;2.
2. Malhi, G. S., Tanious, M. & Gershon, S. The lithiumeter: A measured approach. *Bipolar Disord.* (2011) doi:10.1111/j.1399-5618.2011.00918.x.
3. Pickett, E. E. & O'Dell, B. L. Evidence for dietary essentiality of lithium in the rat. *Biol. Trace Elem. Res.* (1992) doi:10.1007/BF02783685.
4. Schrauzer, G. N. Lithium: Occurrence, Dietary Intakes, Nutritional Essentiality. *J. Am. Coll. Nutr.* (2002) doi:10.1080/07315724.2002.10719188.
5. Brown, E. E., Gerretsen, P., Pollock, B. & Graff-Guerrero, A. Psychiatric benefits of lithium in water supplies may be due to protection from the neurotoxicity of lead exposure. *Med. Hypotheses* (2018) doi:10.1016/j.mehy.2018.04.005.
6. Shorter, E. The history of lithium therapy. *Bipolar Disord.* (2009) doi:10.1111/j.1399-5618.2009.00706.x.
7. Young, W. Review of lithium effects on brain and blood. *Cell Transplant.* **18**, 951–975 (2009).
8. R. D. SHANNON. Revised Effective Ionic Radii and Systematic Studies of Interatomie Distances in Halides and Chaleogenides. *Acta Crystallogr. Sect. A* (1993).
9. Dudev, T., Mazmanian, K. & Lim, C. Competition between Li(+) and Na(+) in sodium transporters and receptors: Which Na(+)-Binding sites are 'therapeutic' Li(+) targets? *Chem. Sci.* **9**, 4093–4103 (2018).
10. De Roos, N. M., De Vries, J. H. M. & Katan, M. B. Serum lithium as a compliance marker for food and supplement in take. *Am. J. Clin. Nutr.* (2001) doi:10.1093/ajcn/73.1.75.
11. Richelson, E. Lithium ion entry through the sodium channel of cultured mouse neuroblastoma cells: A biochemical study. *Science (80-.).* (1977) doi:10.1126/science.860126.
12. Naylor, C. E. *et al.* Molecular basis of ion permeability in a voltage-gated sodium channel. *EMBO J.* (2016) doi:10.15252/embj.201593285.
13. Haas, M., Schooler, J. & Tosteson, D. C. Coupling of lithium to sodium transport in human red cells. *Nature* (1975) doi:10.1038/258425a0.
14. Uwai, Y. *et al.* Sodium-phosphate cotransporter mediates reabsorption of lithium in rat kidney. *Pharmacol. Res.* (2014) doi:10.1016/j.phrs.2014.06.012.
15. Boudker, O., Ryan, R. M., Yernool, D., Shimamoto, K. & Gouaux, E. Coupling substrate and ion binding to extracellular gate of a sodium-dependent aspartate transporter. *Nature* (2007) doi:10.1038/nature05455.
16. Iurinskaia, V. E., Moshkov, A. V, Goriachaia, T. S. & Vereninov, A. A. [Li/Na exchange and Li active transport in human lymphoid cells U937 cultured in lithium media]. *Tsitologiia* **55**, 703–712 (2013).
17. Busch, S., Burckhardt, B. C. & Siffert, W. Expression of the human sodium/proton exchanger NHE-1 in Xenopus laevis oocytes enhances sodium/proton exchange activity and establishes sodium/lithium countertransport. *Pflugers Arch.* **429**, 859–869 (1995).
18. Shalbuyeva, N., Brustovetsky, T. & Brustovetsky, N. Lithium desensitizes brain mitochondria to calcium, antagonizes permeability transition, and diminishes cytochrome

c release. *J. Biol. Chem.* (2007) doi:10.1074/jbc.M702134200.
19. Boyman, L., Williams, G. S. B., Khananshvili, D., Sekler, I. & Lederer, W. J. NCLX: The mitochondrial sodium calcium exchanger. *Journal of Molecular and Cellular Cardiology* (2013) doi:10.1016/j.yjmcc.2013.03.012.
20. Yanagita, T. *et al.* Lithium inhibits function of voltage-dependent sodium channels and catecholamine secretion independent of glycogen synthase kinase-3 in adrenal chromaffin cells. *Neuropharmacology* **53**, 881–889 (2007).
21. Hermans, A. N., Glitsch, H. G. & Verdonck, F. Activation of the Na+/K+ pump current by intra- and extracellular Li ions in single guinea-pig cardiac cells. *Biochim. Biophys. Acta - Biomembr.* **1330**, 83–93 (1997).
22. Thiruvengadam, A. Effect of lithium and sodium valproate ions on resting membrane potentials in neurons: An hypothesis. *J. Affect. Disord.* **65**, 95–99 (2001).
23. Holm, N. G. The significance of Mg in prebiotic geochemistry. *Geobiology* (2012) doi:10.1111/j.1472-4669.2012.00323.x.
24. Dudev, T. & Lim, C. Competition between Li+ and Mg2+ in metalloproteins. Implications for lithium therapy. *J. Am. Chem. Soc.* (2011) doi:10.1021/ja201985s.
25. Dudev, T., Grauffel, C. & Lim, C. How native and alien metal cations bind ATP: Implications for lithium as a therapeutic agent. *Sci. Rep.* **7**, 1–10 (2017).
26. Birch, N. J. LITHIUM AND MAGNESIUM-DEPENDENT ENZYMES. *The Lancet* (1974) doi:10.1016/S0140-6736(74)91187-8.
27. Jakobsson, E. *et al.* Towards a Unified Understanding of Lithium Action in Basic Biology and its Significance for Applied Biology. *Journal of Membrane Biology* (2017) doi:10.1007/s00232-017-9998-2.
28. Avissar, S., Murphy, D. L. & Schreiber, G. Magnesium reversal of lithium inhibition of β-adrenergic and muscarinic receptor coupling to G proteins. *Biochem. Pharmacol.* (1991) doi:10.1016/0006-2952(91)90473-I.
29. Singh, N. *et al.* A safe lithium mimetic for bipolar disorder. *Nat. Commun.* (2013) doi:10.1038/ncomms2320.
30. Brown, K. M. & Tracy, D. K. Lithium: The pharmacodynamic actions of the amazing ion. *Ther. Adv. Psychopharmacol.* (2013) doi:10.1177/2045125312471963.
31. Johnson, S. C. Nutrient sensing, signaling and ageing: The role of IGF-1 and mTOR in ageing and age-related disease. in *Subcellular Biochemistry* (2018). doi:10.1007/978-981-13-2835-0_3.
32. Eng, C. P., Sehgal, S. N. & Vézina, C. Activity of rapamycin (ay-22,989) against transplanted tumors. *J. Antibiot. (Tokyo).* (1984) doi:10.7164/antibiotics.37.1231.
33. Martel, R. R., Klicius, J. & Galet, S. Inhibition of the immune response by rapamycin, a new antifungal antibiotic. *Can. J. Physiol. Pharmacol.* (1977) doi:10.1139/y77-007.
34. Chung, J., Kuo, C. J., Crabtree, G. R. & Blenis, J. Rapamycin-FKBP specifically blocks growth-dependent activation of and signaling by the 70 kd S6 protein kinases. *Cell* (1992) doi:10.1016/0092-8674(92)90643-Q.
35. Saxton, R. A. & Sabatini, D. M. mTOR Signaling in Growth, Metabolism, and Disease. *Cell* (2017) doi:10.1016/j.cell.2017.02.004.
36. LeRoith, D. & Roberts, C. T. The insulin-like growth factor system and cancer. *Cancer Letters* (2003) doi:10.1016/S0304-3835(03)00159-9.
37. Papadopoli, D. *et al.* Mtor as a central regulator of lifespan and aging. *F1000Research* (2019) doi:10.12688/f1000research.17196.1.

38. Oddo, S. The role of mTOR signaling in Alzheimer disease. *Front. Biosci. - Sch.* (2012) doi:10.2741/s310.
39. Zhan, T., Rindtorff, N. & Boutros, M. Wnt signaling in cancer. *Oncogene* (2017) doi:10.1038/onc.2016.304.
40. Inestrosa, N. C. & Toledo, E. M. The role of Wnt signaling in neuronal dysfunction in Alzheimer's Disease. *Molecular Neurodegeneration* (2008) doi:10.1186/1750-1326-3-9.
41. Jia, L., Piña-Crespo, J. & Li, Y. Restoring Wnt/β-catenin signaling is a promising therapeutic strategy for Alzheimer's disease. *Molecular Brain* (2019) doi:10.1186/s13041-019-0525-5.
42. Muneer, A. Wnt and GSK3 signaling pathways in bipolar disorder: Clinical and therapeutic implications. *Clinical Psychopharmacology and Neuroscience* (2017) doi:10.9758/cpn.2017.15.2.100.
43. Machado-Vieira, R., Manji, H. K. & Zarate, C. A. The role of lithium in the treatment of bipolar disorder: Convergent evidence for neurotrophic effects as a unifying hypothesis. *Bipolar Disorders* (2009) doi:10.1111/j.1399-5618.2009.00714.x.
44. Sutherland, C. What are the bona fide GSK3 substrates? *International Journal of Alzheimer's Disease* (2011) doi:10.4061/2011/505607.
45. Hooper, C., Killick, R. & Lovestone, S. The GSK3 hypothesis of Alzheimer's disease. *J. Neurochem.* **104**, 1433–1439 (2008).
46. MacAulay, K. & Woodgett, J. R. Targeting glycogen synthase kinase-3 (GSK-3) in the treatment of Type 2 diabetes. *Expert Opinion on Therapeutic Targets* (2008) doi:10.1517/14728222.12.10.1265.
47. Jope, R. & Roh, M.-S. Glycogen Synthase Kinase-3 (GSK3) in Psychiatric Diseases and Therapeutic Interventions. *Curr. Drug Targets* **7**, 1421–1434 (2012).
48. Domoto, T. *et al.* Glycogen synthase kinase-3β is a pivotal mediator of cancer invasion and resistance to therapy. *Cancer Science* (2016) doi:10.1111/cas.13028.
49. Lee, H.-K., Kumar, P., Fu, Q., Rosen, K. M. & Querfurth, H. W. The insulin/Akt signaling pathway is targeted by intracellular beta-amyloid. *Mol. Biol. Cell* **20**, 1533–1544 (2009).
50. Valvezan, A. J. & Klein, P. S. GSK-3 and Wnt signaling in neurogenesis and bipolar disorder. *Frontiers in Molecular Neuroscience* (2012) doi:10.3389/fnmol.2012.00001.
51. Katoh, M. & Katoh, M. WNT signaling pathway and stem cell signaling network. *Clinical Cancer Research* (2007) doi:10.1158/1078-0432.CCR-06-2316.
52. Nusse, R. & Clevers, H. Wnt/β-Catenin Signaling, Disease, and Emerging Therapeutic Modalities. *Cell* (2017) doi:10.1016/j.cell.2017.05.016.
53. Magdesian, M. H. *et al.* Amyloid-β binds to the extracellular cysteine-rich domain of frizzled and inhibits Wnt/β-catenin signaling. *J. Biol. Chem.* (2008) doi:10.1074/jbc.M707108200.
54. Tapia-Rojas, C., Burgos, P. V. & Inestrosa, N. C. Inhibition of Wnt signaling induces amyloidogenic processing of amyloid precursor protein and the production and aggregation of Amyloid-β (Aβ)42 peptides. *J. Neurochem.* (2016) doi:10.1111/jnc.13873.
55. Zilka, N. & Novak, M. The tangled story of Alois Alzheimer. *Bratisl. Lek. Listy* **107**, 343–345 (2006).
56. Yamazaki, Y., Zhao, N., Caulfield, T. R., Liu, C. C. & Bu, G. Apolipoprotein E and Alzheimer disease: pathobiology and targeting strategies. *Nature Reviews Neurology* (2019) doi:10.1038/s41582-019-0228-7.

57. Dhana, K., Evans, D. A., Rajan, K. B., Bennett, D. A. & Morris, M. C. Healthy lifestyle and the risk of Alzheimer dementia: Findings from 2 longitudinal studies. *Neurology* (2020) doi:10.1212/WNL.0000000000009816.
58. Ramos-Cejudo, J. *et al.* Traumatic Brain Injury and Alzheimer's Disease: The Cerebrovascular Link. *EBioMedicine* (2018) doi:10.1016/j.ebiom.2018.01.021.
59. Naughton, S. X., Raval, U. & Pasinetti, G. M. The viral hypothesis in alzheimer's disease: Novel insights and pathogen-based biomarkers. *Journal of Personalized Medicine* (2020) doi:10.3390/jpm10030074.
60. Tanzi, R. E. & Bertram, L. Twenty years of the Alzheimer's disease amyloid hypothesis: A genetic perspective. *Cell* **120**, 545–555 (2005).
61. Rygiel, K. Novel strategies for Alzheimer's disease treatment: An overview of anti-amyloid beta monoclonal antibodies. *Indian Journal of Pharmacology* (2016) doi:10.4103/0253-7613.194867.
62. Christensen, D. D. Changing the course of Alzheimer's disease: Anti-amyloid disease-modifying treatments on the horizon. *Primary Care Companion to the Journal of Clinical Psychiatry* (2007) doi:10.4088/pcc.v09n0106.
63. Irizarry, M. C., McNamara, M., Fedorchak, K., Hsiao, K. & Hyman, B. T. APPsw Transgenic Mice Develop Age-related Aβ Deposits and Neuropil Abnormalities, but no Neuronal Loss in CA1. *J. Neuropathol. Exp. Neurol.* **56**, 965–973 (1997).
64. Davinelli, S. *et al.* The 'Alzheimer's disease signature': Potential perspectives for novel biomarkers. *Immun. Ageing* **8**, 7 (2011).
65. Carrillo-Mora, P., Luna, R. & Colín-Barenque, L. Amyloid beta: Multiple mechanisms of toxicity and only some protective effects? *Oxid. Med. Cell. Longev.* **2014**, (2014).
66. Kim, J. *et al.* Normal cognition in transgenic BRI2-Aβ mice. *Mol. Neurodegener.* (2013) doi:10.1186/1750-1326-8-15.
67. Morroni, F., Sita, G., Tarozzi, A., Rimondini, R. & Hrelia, P. Early effects of Aβ1-42 oligomers injection in mice: Involvement of PI3K/Akt/GSK3 and MAPK/ERK1/2 pathways. *Behav. Brain Res.* (2016) doi:10.1016/j.bbr.2016.08.002.
68. Balducci, C. *et al.* Synthetic amyloid-β oligomers impair long-term memory independently of cellular prion protein. *Proc. Natl. Acad. Sci. U. S. A.* (2010) doi:10.1073/pnas.0911829107.
69. Kametani, F. & Hasegawa, M. Reconsideration of amyloid hypothesis and tau hypothesis in Alzheimer's disease. *Front. Neurosci.* **12**, (2018).
70. Ittner, L. M. *et al.* Dendritic function of tau mediates amyloid-β toxicity in alzheimer's disease mouse models. *Cell* (2010) doi:10.1016/j.cell.2010.06.036.
71. Musiek, E. S. & Holtzman, D. M. Three dimensions of the amyloid hypothesis: Time, space and 'wingmen'. *Nature Neuroscience* (2015) doi:10.1038/nn.4018.
72. Counts, S. E., Ikonomovic, M. D., Mercado, N., Vega, I. E. & Mufson, E. J. Biomarkers for the Early Detection and Progression of Alzheimer's Disease. *Neurotherapeutics* **14**, 35–53 (2017).
73. Khan, T. K. *Biomarkers in Alzheimer's Disease*. *Biomarkers in Alzheimer's Disease* (2016). doi:10.18679/cn11-6030_r.2016.002.
74. Takashima, A. GSK-3 is essential in the pathogenesis of Alzheimer's disease. *Journal of Alzheimer's Disease* (2006) doi:10.3233/jad-2006-9s335.
75. Hernandez, F., Lucas, J. J. & Avila, J. GSK3 and tau: Two convergence points in Alzheimer's disease. *Journal of Alzheimer's Disease* (2013) doi:10.3233/JAD-2012-

129025.
76. Krishnankutty, A. *et al.* In vivo regulation of glycogen synthase kinase 3β activity in neurons and brains. *Sci. Rep.* (2017) doi:10.1038/s41598-017-09239-5.
77. Beurel, E., Grieco, S. F. & Jope, R. S. Glycogen synthase kinase-3 (GSK3): Regulation, actions, and diseases. *Pharmacology and Therapeutics* (2015) doi:10.1016/j.pharmthera.2014.11.016.
78. Cross, D. A. E., Alessi, D. R., Cohen, P., Andjelkovich, M. & Hemmings, B. A. Inhibition of glycogen synthase kinase-3 by insulin mediated by protein kinase B. *Nature* (1995) doi:10.1038/378785a0.
79. Fang, X. *et al.* Phosphorylation and inactivation of glycogen synthase kinase 3 by protein kinase A. *Proc. Natl. Acad. Sci. U. S. A.* (2000) doi:10.1073/pnas.220413597.
80. Zhou, X., Wang, H., Burg, M. B. & Ferraris, J. D. Inhibitory phosphorylation of GSK-3β by AKT, PKA, and PI3K contributes to high NaCl-induced activation of the transcription factor NFAT5 (TonEBP/OREBP). *Am. J. Physiol. - Ren. Physiol.* (2013) doi:10.1152/ajprenal.00591.2012.
81. Goode, N., Hughes, K., Woodgett, J. R. & Parker, P. J. Differential regulation of glycogen synthase kinase-3β by protein kinase C isotypes. *J. Biol. Chem.* (1992).
82. Martinez, A. & Perez, D. GSK-3 Inhibitors: A Ray of Hope for the Treatment of Alzheimer's Disease? *J. Alzheimers. Dis.* **15**, 181–191 (2008).
83. Yamaguchi, H. *et al.* Preferential labeling of Alzheimer neurofibrillary tangles with antisera for tau protein kinase (TPK) I/glycogen synthase kinase-3β and cyclin-dependent kinase 5, a component of TPK II. *Acta Neuropathol.* (1996) doi:10.1007/s004010050513.
84. Leroy, K., Yilmaz, Z. & Brion, J. P. Increased level of active GSK-3β in Alzheimer's disease and accumulation in argyrophilic grains and in neurones at different stages of neurofibrillary degeneration. *Neuropathol. Appl. Neurobiol.* (2007) doi:10.1111/j.1365-2990.2006.00795.x.
85. Blalock, E. M. *et al.* Incipient Alzheimer's disease: Microarray correlation analyses reveal major transcriptional and tumor suppressor responses. *Proc. Natl. Acad. Sci. U. S. A.* (2004) doi:10.1073/pnas.0308512100.
86. Turenne, G. A. & Price, B. D. Glycogen synthase kinase3 beta phosphorylates serine 33 of p53 and activates p53's transcriptional activity. *BMC Cell Biol.* (2001) doi:10.1186/1471-2121-2-12.
87. Xing, B., Li, Y. C. & Gao, W. J. GSK3β Hyperactivity during an Early Critical Period Impairs Prefrontal Synaptic Plasticity and Induces Lasting Deficits in Spine Morphology and Working Memory. *Neuropsychopharmacology* (2016) doi:10.1038/npp.2016.110.
88. Lim, N. K. H. *et al.* Localized changes to glycogen synthase kinase-3 and collapsin response mediator protein-2 in the Huntington's disease affected brain. *Hum. Mol. Genet.* (2014) doi:10.1093/hmg/ddu119.
89. Fernández-Nogales, M. *et al.* Decreased glycogen synthase kinase-3 levels and activity contribute to Huntington's disease. *Hum. Mol. Genet.* (2015) doi:10.1093/hmg/ddv224.
90. Matsunaga, S. *et al.* Lithium as a Treatment for Alzheimer's Disease: A Systematic Review and Meta-Analysis. *J. Alzheimer's Dis.* **48**, 403–410 (2015).
91. Zhang, X. *et al.* Long-term treatment with lithium alleviates memory deficits and reduces amyloid-β production in an aged Alzheimer's disease transgenic mouse model. *J. Alzheimer's Dis.* **24**, 739–749 (2011).
92. Caccamo, A., Oddo, S., Tran, L. X. & LaFerla, F. M. Lithium reduces tau phosphorylation

but not Aβ or working memory deficits in a transgenic model with both plaques and tangles. *Am. J. Pathol.* **170**, 1669–1675 (2007).
93. Wagner, U., Utton, M., Gallo, J. M. & Miller, C. C. J. Cellular phosphorylation of tau by GSK-3β influences tau binding to microtubules and microtubule organisation. *J. Cell Sci.* **109**, 1537–1543 (1996).
94. De Ferrari, G. V. *et al.* Activation of Wnt signaling rescues neurodegeneration and behavioral impairments induced by β-amyloid fibrils. *Mol. Psychiatry* (2003) doi:10.1038/sj.mp.4001208.
95. De-Paula, V. J., Gattaz, W. F. & Forlenza, O. V. Long-term lithium treatment increases intracellular and extracellular brain-derived neurotrophic factor (BDNF) in cortical and hippocampal neurons at subtherapeutic concentrations. *Bipolar Disord.* (2016) doi:10.1111/bdi.12449.
96. Zhu, Z. *et al.* Lithium stimulates human bone marrow derived mesenchymal stem cell proliferation through GSK-3β-dependent β-catenin/Wnt pathway activation. *FEBS J.* (2014) doi:10.1111/febs.13081.
97. Zhang, J., He, L., Yang, Z., Li, L. & Cai, W. Lithium chloride promotes proliferation of neural stem cells in vitro, possibly by triggering the Wnt signaling pathway. *Animal Cells Syst. (Seoul).* (2019) doi:10.1080/19768354.2018.1487334.
98. Hee, J. K. & Thayer, S. A. Lithium increases synapse formation between hippocampal neurons by depleting phosphoinositides. *Mol. Pharmacol.* (2009) doi:10.1124/mol.108.052357.
99. Chen, G., Rajkowska, G., Du, F., Seraji-Bozorgzad, N. & Manji, H. K. Enhancement of hippocampal neurogenesis by lithium. *J. Neurochem.* (2000) doi:10.1046/j.1471-4159.2000.0751729.x.
100. Fiorentini, A., Rosi, M. C., Grossi, C., Luccarini, I. & Casamenti, F. Lithium improves hippocampal neurogenesis, neuropathology and cognitive functions in APP mice. *PLoS One* (2010) doi:10.1371/journal.pone.0014382.
101. Jackson, W. C. A Historical Dictionary of Psychiatry. *Prim. Care Companion J. Clin. Psychiatry* (2006) doi:10.4088/pcc.v08n0511.
102. Merikangas, K. R. *et al.* Prevalence and correlates of bipolar spectrum disorder in the World Mental Health Survey Initiative. *Arch. Gen. Psychiatry* (2011) doi:10.1001/archgenpsychiatry.2011.12.
103. Anderson, I. M., Haddad, P. M. & Scott, J. Bipolar disorder. *BMJ* **345**, 1–10 (2012).
104. Miklowitz, D. J. & Johnson, S. L. The psychopathology and treatment of bipolar disorder. *Annual Review of Clinical Psychology* (2006) doi:10.1146/annurev.clinpsy.2.022305.095332.
105. Luykx, J. J. *et al.* The involvement of GSK3β in bipolar disorder: Integrating evidence from multiple types of genetic studies. *European Neuropsychopharmacology* (2010) doi:10.1016/j.euroneuro.2010.02.008.
106. Sahin, C., Unal, G. & Aricioglu, F. Regulation of GSK-3 Activity as A Shared Mechanism in Psychiatric Disorders. *Klin. Psikofarmakol. Bülteni-Bulletin Clin. Psychopharmacol.* (2014) doi:10.5455/bcp.20140317063255.
107. Shioya, A. *et al.* Neurodegenerative changes in patients with clinical history of bipolar disorders. *Neuropathology* (2015) doi:10.1111/neup.12191.
108. Iwahashi, K. *et al.* Haplotype analysis of GSK-3β gene polymorphisms in bipolar disorder lithium responders and nonresponders. *Clin. Neuropharmacol.* (2014)

doi:10.1097/WNF.0000000000000039.
109. Manji, H. K. *et al.* The underlying neurobiology of bipolar disorder. *World Psychiatry* **2**, 136–46 (2003).
110. Malhi, G. S., Gessler, D. & Outhred, T. The use of lithium for the treatment of bipolar disorder: Recommendations from clinical practice guidelines. *J. Affect. Disord.* (2017) doi:10.1016/j.jad.2017.03.052.
111. Kurita, M. Noradrenaline plays a critical role in the switch to a manic episode and treatment of a depressive episode. *Neuropsychiatr. Dis. Treat.* **12**, 2373–2380 (2016).
112. Rotondo, A. *et al.* Catechol O-methyltransferase, serotonin transporter, and tryptophan hydroxylase gene polymorphisms in bipolar disorder patients with and without comorbid panic disorder. *Am. J. Psychiatry* (2002) doi:10.1176/appi.ajp.159.1.23.
113. Kirov, G. *et al.* Low activity allele of catechol-O-methyltransferase gene associated with rapid cycling bipolar disorder. *Mol. Psychiatry* (1998) doi:10.1038/sj.mp.4000385.
114. Wolf, M. A., Louis, J.-C. & Vincendon, G. Antidepressant effect of lithium: A neurochemical study on neuronal uptake of norepinephrine and serotonin. *Prog. Neuropsychopharmacol. Biol. Psychiatry* **13**, 765–773 (1989).
115. Devaki, R., Rao, S. S. & Nadgir, S. M. The effect of lithium on the adrenoceptor-mediated second messenger system in the rat brain. *J. Psychiatry Neurosci.* **31**, 246–252 (2006).
116. Bhatia, A. & Saadabadi, A. *Biochemistry, Dopamine Receptors*. *StatPearls* (2019).
117. Howes, O. *et al.* Mechanisms Underlying Psychosis and Antipsychotic Treatment Response in Schizophrenia: Insights from PET and SPECT Imaging. *Curr. Pharm. Des.* (2009) doi:10.2174/138161209788957528.
118. Li, Y. C., Xi, D., Roman, J., Huang, Y. Q. & Gao, W. J. Activation of glycogen synthase kinase-3β is required for hyperdopamine and D2 receptor-mediated inhibition of synaptic NMDA receptor function in the rat prefrontal cortex. *J. Neurosci.* (2009) doi:10.1523/JNEUROSCI.3336-09.2009.
119. Manji, H. K. & Chen, G. PKC, MAP kinases and the bcl-2 family of proteins as long-term targets for mood stabilizers. *Mol. Psychiatry* (2002) doi:10.1038/sj/mp/4001018.
120. Drevets, W. C. *et al.* Serotonin-1A receptor imaging in recurrent depression: replication and literature review. *Nucl. Med. Biol.* **34**, 865–877 (2007).
121. Price, L. H., Charney, D. S., Delgado, P. L. & Heninger, G. R. Lithium and serotonin function: implications for the serotonin hypothesis of depression. *Psychopharmacology* (1990) doi:10.1007/BF02245781.
122. Nugent, A. C. *et al.* Mood stabilizer treatment increases serotonin type 1A receptor binding in bipolar depression. *J. Psychopharmacol.* (2013) doi:10.1177/0269881113499204.
123. Van Enkhuizen, J. *et al.* The catecholaminergic-cholinergic balance hypothesis of bipolar disorder revisited. *Eur. J. Pharmacol.* (2015) doi:10.1016/j.ejphar.2014.05.063.
124. Jope, R. S. EFFECTS OF LITHIUM TREATMENT IN VITRO AND IN VIVO ON ACETYLCHOLINE METABOLISM IN RAT BRAIN. *J. Neurochem.* (1979) doi:10.1111/j.1471-4159.1979.tb05179.x.
125. Van Enkhuizen, J., Milienne-Petiot, M., Geyer, M. A. & Young, J. W. Modeling bipolar disorder in mice by increasing acetylcholine or dopamine: Chronic lithium treats most, but not all features. *Psychopharmacology (Berl).* (2015) doi:10.1007/s00213-015-4000-4.
126. Malhi, G. S., Tanious, M., Das, P., Coulston, C. M. & Berk, M. Potential mechanisms of action of lithium in bipolar disorder: Current understanding. *CNS Drugs* (2013)

doi:10.1007/s40263-013-0039-0.
127. Motohashi, N. GABA receptor alterations after chronic lithium administration. Comparison with carbamazepine and sodium valproate. *Prog. Neuropsychopharmacol. Biol. Psychiatry* (1992) doi:10.1016/0278-5846(92)90062-J.
128. Motohashi, N., Ikawa, K. & Kariya, T. GABAB receptors are up-regulated by chronic treatment with lithium or carbamazepine. GABA hypothesis of affective disorders? *Eur. J. Pharmacol.* (1989) doi:10.1016/0014-2999(89)90687-0.
129. Baldessarini, R. J. *et al.* Decreased risk of suicides and attempts during long-term lithium treatment: A meta-analytic review. *Bipolar Disorders* (2006) doi:10.1111/j.1399-5618.2006.00344.x.
130. Goodwin, F. K. *et al.* Suicide Risk in Bipolar Disorder during Treatment with Lithium and Divalproex. *J. Am. Med. Assoc.* (2003) doi:10.1001/jama.290.11.1467.
131. Dwivedi, T. & Zhang, H. Lithium-induced neuroprotection is associated with epigenetic modification of specific BDNF gene promoter and altered expression of apoptotic-regulatory proteins. *Front. Neurosci.* (2015) doi:10.3389/fnins.2014.00457.
132. Berk, M. Neuroprogression: Pathways to progressive brain changes in bipolar disorder. *International Journal of Neuropsychopharmacology* (2009) doi:10.1017/S1461145708009498.
133. Quiroz, J. A., MacHado-Vieira, R., Zarate, C. A. & Manji, H. K. Novel insights into lithium's mechanism of action: Neurotrophic and neuroprotective effects. *Neuropsychobiology* (2010) doi:10.1159/000314310.
134. Lieberman, K., Alexander, G. J. & Sechzer, J. A. Stable isotopes of lithium: dissimilar biochemical and behavioral effects. *Experientia* **42**, 985–987 (1986).
135. Sechzer, J. A., Lieberman, K. W., Alexander, G. J., Weidman, D. & Stokes, P. E. Aberrant parenting and delayed offspring development in rats exposed to lithium. *Biol. Psychiatry* **21**, 1258–1266 (1986).
136. Alexander, G. J., Lieberman, K. W. & Stokes, P. Differential lethality of lithium isotopes in mice. *Biol. Psychiatry* (1980).
137. PARTHASARATHY, R. & EISENBERG, F. Lack of Differential Lethality of Lithium Isotopes in Mice. *Ann. N. Y. Acad. Sci.* (1984) doi:10.1111/j.1749-6632.1984.tb13853.x.
138. Lieberman, K. W., Alexander, G. J. & Stokes, P. Dissimilar effects of lithium isotopes on motility in rats. *Pharmacol. Biochem. Behav.* **10**, 933–935 (1979).
139. Sherman, W. R., Munsell, L. Y. & Wong, Y. H. Differential Uptake of Lithium Isotopes by Rat Cerebral Cortex and Its Effect on Inositol Phosphate Metabolism. *J. Neurochem.* **42**, 880–882 (1984).
140. Svishchev, I. M. & Kusalik, P. G. Dynamics in liquid water, water-d2, and water-t2: a comparative simulation study. *J. Phys. Chem.* **98**, 728–733 (1994).
141. Lamprecht, J., Schroeter, D. & Paweletz, N. Derangement of microtubule arrays in interphase and mitotic PtK2 cells treated with deuterium oxide (heavy water). *J. Cell Sci.* (1991).
142. Bild, W., Nastasa, V. & Haulica, I. In vivo and in vitro research on the biological effects of deuterium-depleted water: 1. Influence of deuterium-depleted water on cultured cell growth. *Rom. J. Physiol.* (2004).
143. Kushner, D. J., Baker, A. & Dunstall, T. G. Pharmacological uses and perspectives of heavy water and deuterated compounds. *Canadian Journal of Physiology and Pharmacology* (1999) doi:10.1139/y99-005.

144. Roth, J. P. & Klinman, J. P. Kinetic Isotope Effects. in *Encyclopedia of Biological Chemistry: Second Edition* (2013). doi:10.1016/B978-0-12-378630-2.00016-5.
145. Wang, Y. *et al.* Magnesium isotope fractionation reflects plant response to magnesium deficiency in magnesium uptake and allocation: a greenhouse study with wheat. *Plant Soil* (2020) doi:10.1007/s11104-020-04604-2.
146. Hayes, J. M. Fractionation of carbon and hydrogen isotopes in biosynthetic processes. *Rev. Mineral. Geochemistry* (2001) doi:10.2138/gsrmg.43.1.225.
147. Karandashev, K., Xu, Z. H., Meuwly, M., Vaníček, J. & Richardson, J. O. Kinetic isotope effects and how to describe them. *Structural Dynamics* (2017) doi:10.1063/1.4996339.
148. Trixler, F. Quantum Tunnelling to the Origin and Evolution of Life. *Curr. Org. Chem.* (2013) doi:10.2174/13852728113179990083.
149. Qaswal, A. B. Lithium Stabilizes the Mood of Bipolar Patients by Depolarizing the Neuronal Membrane Via Quantum Tunneling through the Sodium Channels. *Clin. Psychopharmacol. Neurosci.* (2020) doi:10.9758/cpn.2020.18.2.214.
150. Barjas Qaswal, A. Quantum Tunneling of Ions through the Closed Voltage-Gated Channels of the Biological Membrane: A Mathematical Model and Implications. *Quantum Reports* (2019) doi:10.3390/quantum1020019.
151. Barjas Qaswal, A. Magnesium Ions Depolarize the Neuronal Membrane via Quantum Tunneling through the Closed Channels. *Quantum Reports* (2020) doi:10.3390/quantum2010005.
152. Fisher, M. P. A. Quantum cognition: The possibility of processing with nuclear spins in the brain. *Ann. Phys. (N. Y).* **362**, 593–602 (2015).
153. Player, T. C., Hore, P. J. & Category, S. Posner qubits: Spin dynamics of entangled Ca9(PO4)6 molecules and their role in neural processing. *J. R. Soc. Interface* (2018) doi:10.1098/rsif.2018.0494.
154. Weingarten, C. P., Doraiswamy, P. M. & Fisher, M. P. A. A new spin on neural processing: Quantum cognition. *Frontiers in Human Neuroscience* (2016) doi:10.3389/fnhum.2016.00541.
155. Ettenberg, A. *et al.* Differential effects of lithium isotopes in a ketamine-induced hyperactivity model of mania. *Pharmacol. Biochem. Behav.* (2020) doi:10.1016/j.pbb.2020.172875.
156. Li, N. *et al.* Nuclear Spin Attenuates the Anesthetic Potency of Xenon Isotopes in Mice. *Anesthesiology* (2018) doi:10.1097/aln.0000000000002226.
157. Scherer, W. F., Syverton, J. T. & Gey, G. O. Studies on the propagation in vitro of poliomyelitis viruses: IV. Viral multiplication in a stable strain of human malignant epithelial cells (strain hela) derived from an epidermoid carcinoma of the cervix. *J. Exp. Med.* (1953) doi:10.1084/jem.97.5.695.
158. Steele, S. L. *et al.* Telomerase immortalization of principal cells from mouse collecting duct. *Am. J. Physiol. - Ren. Physiol.* (2010) doi:10.1152/ajprenal.00183.2010.
159. Jha, K. K., Banga, S., Palejwala, V. & Ozer, H. L. SV40-mediated immortalization. *Exp. Cell Res.* (1998) doi:10.1006/excr.1998.4272.
160. Morimoto, B. H. & Koshland, D. E. Induction and expression of long- and short-term neurosecretory potentiation in a neural cell line. *Neuron* (1990) doi:10.1016/0896-6273(90)90347-I.
161. He, M., Liu, J., Cheng, S., Xing, Y. & Suo, W. Z. Differentiation renders susceptibility to excitotoxicity in HT22 neurons. *Neural Regen. Res.* **8**, 1297–1306 (2013).

162. Liu, J., Li, L. & Suo, W. Z. HT22 hippocampal neuronal cell line possesses functional cholinergic properties. *Life Sci.* (2009) doi:10.1016/j.lfs.2008.12.008.
163. Mu, Y. & Gage, F. H. Adult hippocampal neurogenesis and its role in Alzheimer's disease. *Molecular Neurodegeneration* (2011) doi:10.1186/1750-1326-6-85.
164. Martínez, E., Navarro, A., Ordóez, C., Del Valle, E. & Tolivia, J. Amyloid-β25-35 induces apolipoprotein D synthesis and growth arrest in HT22 hippocampal cells. *J. Alzheimer's Dis.* (2012) doi:10.3233/JAD-2012-112102.
165. Hogins, J., Crawford, D. C., Zorumski, C. F. & Mennerick, S. Excitotoxicity triggered by neurobasal culture medium. *PLoS One* (2011) doi:10.1371/journal.pone.0025633.
166. Figueroa, J. A. L., Stiner, C. A., Radzyukevich, T. L. & Heiny, J. A. Metal ion transport quantified by ICP-MS in intact cells. *Sci. Rep.* (2016) doi:10.1038/srep20551.
167. Wilschefski, S. & Baxter, M. Inductively Coupled Plasma Mass Spectrometry: Introduction to Analytical Aspects. *Clin. Biochem. Rev.* (2019) doi:10.33176/aacb-19-00024.
168. Allen, R. & Gilstrap, J. A colloidal nanoparticle form of indium tin oxide: system development and characterization. *J. Chem. Inf. Model.* (2009) doi:10.1017/CBO9781107415324.004.
169. Riss, T. L. *et al. Cell Viability Assays*. *Assay Guidance Manual* (2004).
170. Huang, Y. *et al.* Lithium prevents acrolein-induced neurotoxicity in HT22 mouse hippocampal Cells. *Neurochem. Res.* (2014) doi:10.1007/s11064-014-1252-z.
171. Zegzouti, H., Zdanovskaia, M., Hsiao, K. & Goueli, S. A. ADP-Glo: A bioluminescent and homogeneous adp monitoring assay for Kinases. *Assay Drug Dev. Technol.* (2009) doi:10.1089/adt.2009.0222.
172. Klein, P. S. & Melton, D. A. A molecular mechanism for the effect of lithium on development. *Proc. Natl. Acad. Sci. U. S. A.* (1996) doi:10.1073/pnas.93.16.8455.
173. Ryves, W. J. & Harwood, A. J. Lithium inhibits glycogen synthase kinase-3 by competition for magnesium. *Biochem. Biophys. Res. Commun.* (2001) doi:10.1006/bbrc.2000.4169.
174. Scarpa, A. & Brinley, F. J. In situ measurements of free cytosolic magnesium ions. *Fed. Proc.* (1981).
175. Romani, A. & Scarpa, A. Regulation of cell magnesium. *Arch. Biochem. Biophys.* (1992) doi:10.1016/0003-9861(92)90086-C.
176. Towbin, H., Staehelin, T. & Gordon, J. Electrophoretic transfer of proteins from polyacrylamide gels to nitrocellulose sheets: Procedure and some applications. *Proc. Natl. Acad. Sci. U. S. A.* (1979) doi:10.1073/pnas.76.9.4350.
177. Monaco, S. A., Ferguson, B. R. & Gao, W. J. Lithium inhibits GSK3β and augments GluN2A receptor expression in the prefrontal cortex. *Front. Cell. Neurosci.* (2018) doi:10.3389/fncel.2018.00016.
178. de Sousa, R. T. *et al.* Lithium increases platelet serine-9 phosphorylated GSK-3β levels in drug-free bipolar disorder during depressive episodes. *J. Psychiatr. Res.* (2015) doi:10.1016/j.jpsychires.2015.01.016.
179. Hallcher, L. M. & Sherman, W. R. The effects of lithium ion and other agents on the activity of myo-inositol-1-phosphatase from bovine brain. *J. Biol. Chem.* (1980).

		6 -> 6 Li [He]		7 -> 7 Li [He]		mol/mL total Li	6Li mol/mL	6Li ng/mL	mol/mL total Li	7Li mol/mL	7Li ng/mL	Dilution Factor	Dilution-corrected 6Li	Dilution-corrected 7Li	7Li/6Li	7Li	6Li	
Sample Name	Vial Number	Conc. [ng/ml]	Conc. RSD	Conc. [ng/ml]	Conc. RSD	(using 6Li)			(using 7Li)				Conc. [ng/ml]	Conc. [ng/ml]		%	%	
Procedural Blank	2512	1.0	174.8	0.3	18.0	1.4E-10	1.1E-11	6.4E-02	3.6E-11	3.3E-11	2.3E-01	10	0.64	2.3	(total procedural blank in Q and R)			
Procedural Blank	2512	4.6	57.6	3.3	11.7	6.7E-10	5.1E-11	3.0E-01	4.7E-10	4.4E-10	3.1E+00	10	3.0	31	(total procedural blank in Q and R)			
Sample 1	2109	870.0	18.5	843.3	18.1	1.3E-07	9.5E-09	5.7E+01	1.2E-07	1.1E-07	7.9E+02	29.0	1660	22846	11.80	92.2	7.8	10cm plate media Li7
Sample 1 - rpt	2101	7610.4	23.1	7592.2	23.0	1.1E-06	8.3E-08	5.0E+02	1.1E-06	1.0E-06	7.1E+03	2.9	1453	20581	12.15	92.4	7.6	10cm plate media Li7
Sample 2	2101	683.0	3.2	627.2	2.8	9.8E-08	7.5E-09	4.5E+01	9.0E-08	8.4E-08	5.9E+02	0.7	33	427	11.18	91.8	8.2	10cm plate PBS Wash Li7
Sample 2 - rpt	2102	649.0	3.1	688.7	0.8	9.4E-08	7.1E-09	4.3E+01	9.9E-08	9.2E-08	6.4E+02	0.7	31	468	12.92	92.8	7.2	10cm plate PBS Wash Li7
Sample 2 - rpt2	2102	565.8	8.5	637.5	9.7	8.2E-08	6.2E-09	3.7E+01	9.2E-08	8.5E-08	6.0E+02	0.7	27	434	13.72	93.2	6.8	10cm plate PBS Wash Li7
Sample 3	2102	455.1	9.3	129.6	9.3	6.6E-08	5.0E-09	3.0E+01	1.9E-08	1.7E-08	1.2E+02	2.4	73	294	3.47	77.6	22.4	10cm plate cells 4mmol Li7
Sample 3 - rpt	2103	604.4	5.9	169.5	6.1	8.7E-08	6.6E-09	4.0E+01	2.4E-08	2.3E-08	1.6E+02	2.4	97	385	3.41	77.3	22.7	10cm plate cells 4mmol Li7
Sample 3 - rpt2	2103	440.8	1.5	127.9	0.4	6.4E-08	4.8E-09	2.9E+01	1.8E-08	1.7E-08	1.2E+02	2.4	70	290	3.53	77.9	22.1	10cm plate cells 4mmol Li7
Sample 4	2104	29.8	12.6	4.1	5.3	4.3E-09	3.3E-10	2.0E+00	5.9E-10	5.4E-10	3.8E+00	2.4	4.7	9.1	1.66	62.4	37.6	10cm plate media cells control
Sample 5	2105	18.7	37.3	2.7	27.1	2.7E-09	2.0E-10	1.2E+00	3.8E-10	3.5E-10	2.5E+00	2.3	2.8	5.6	1.73	63.3	36.7	10cm plate media control
Sample 6	2103	1049.0	6.1	78.0	4.7	1.5E-07	1.1E-08	6.9E+01	1.1E-08	1.0E-08	7.3E+01	2.1	146	154	0.91	47.5	52.5	10cm plate 4mmol cells Li6
Sample 6 - rpt	2106	922.4	3.9	65.4	1.2	1.3E-07	1.0E-08	6.1E+01	9.4E-09	8.7E-09	6.1E+01	2.1	128	129	0.86	46.3	53.7	10cm plate 4mmol cells Li6
Sample 6 - rpt2	2106	679.0	2.2	46.3	1.9	9.8E-08	7.4E-09	4.5E+01	6.7E-09	6.2E-09	4.3E+01	2.1	94	91	0.83	45.4	54.6	10cm plate 4mmol cells Li6
Sample 7	2110	2170.9	4.9	14.6	7.7	3.1E-07	2.4E-08	1.4E+02	2.1E-09	1.9E-09	1.4E+01	11.1	1579	151	0.08	7.6	92.4	10cm plate PBS wash 4mmol Li6
Sample 7 - rpt	2107	16236.2	1.6	64.3	1.5	2.3E-06	1.8E-07	1.1E+03	9.3E-09	8.6E-09	6.0E+01	1.1	1175	66	0.05	4.6	95.4	10cm plate PBS wash 4mmol Li6
Sample 8	2104	1250.9	1.2	8.8	3.6	1.8E-07	1.4E-08	8.2E+01	1.3E-09	1.2E-09	8.2E+00	255.6	21034	2102	0.09	7.9	92.1	10cm plate 4mmol media Li6
Sample 8 - rpt	2108	129611.7	0.9	477.3	1.4	1.9E-05	1.4E-06	8.5E+03	6.9E-08	6.4E-08	4.5E+02	2.5	21466	1123	0.04	4.3	95.7	10cm plate 4mmol media Li6
Sample 9	2109	8.4	16.4	1.0	4.8	1.2E-09	9.2E-11	5.5E-01	1.4E-10	1.3E-10	9.0E-01	10.6	5.9	9.6	1.41	58.4	41.6	4mmol lysis buffer C
Sample 10	2110	112.3	12.4	1.9	5.0	1.6E-08	1.2E-09	7.4E+00	2.7E-10	2.5E-10	1.8E+00	10.3	76	18	0.21	17.1	82.9	4mmol lysis buffer 6
Sample 11	2111	13.0	7.1	9.2	2.8	1.9E-09	1.4E-10	8.5E-01	1.3E-09	1.2E-09	8.6E+00	10.4	8.9	90	8.66	89.7	10.3	4mmol lysis buffer 7
Sample 12	2112	3.6	58.8	0.7	15.0	5.2E-10	3.9E-11	2.4E-01	9.9E-11	9.1E-11	6.4E-01	11.6	2.7	7.4	2.32	69.9	30.1	trypsin #1 Cells C1
Sample 13	2201	103.2	7.6	1.1	8.5	1.5E-08	1.1E-09	6.8E+00	1.6E-10	1.5E-10	1.0E+00	11.3	77	12	0.13	11.6	88.4	Trypsin #1 Cells 4mmol Li6
Sample 14	2202	11.6	16.1	7.9	8.3	1.7E-09	1.3E-10	7.6E-01	1.1E-09	1.1E-09	7.4E+00	11.6	8.8	86	8.36	89.3	10.7	Trypsin #1 Cells 4mmol Li7
Sample 15	2203	3.1	37.8	0.7	19.3	4.4E-10	3.4E-11	2.0E-01	1.0E-10	9.7E-11	6.8E-01	13.0	2.6	8.8	2.88	74.2	25.8	Trypsin #1 cells C2
Sample 16	2112	22099.1	3.3	86.4	3.1	3.2E-06	2.4E-07	1.5E+03	1.2E-08	1.1E-08	8.1E+01	12.4	18056	1002	0.05	4.5	95.5	Trypsin #1 media 4mmol Li6
Sample 16 - rpt	2204	29307.8	1.1	112.1	0.2	4.2E-06	3.2E-07	1.9E+03	1.6E-08	1.5E-08	1.0E+02	12.4	23946	1300	0.05	4.4	95.6	Trypsin #1 media 4mmol Li6
Sample 17	2105	2119.0	10.8	2041.1	9.9	3.1E-07	2.3E-08	1.4E+02	2.9E-07	2.7E-07	1.9E+03	12.6	1751	23954	11.73	92.1	7.9	Trypsin #1 media 4mmol Li7
Sample 17 - rpt	2205	1989.3	19.1	1937.7	18.4	2.9E-07	2.2E-08	1.3E+02	2.8E-07	2.6E-07	1.8E+03	12.6	1644	22741	11.86	92.2	7.8	Trypsin #1 media 4mmol Li7
Sample 18	2206	3.6	26.5	0.7	10.8	5.1E-10	3.9E-11	2.3E-01	9.6E-11	8.8E-11	6.2E-01	12.4	2.9	7.7	2.27	69.5	30.5	Trypsin #2 Cells C
Sample 19	2207	28.8	10.1	11.9	5.9	4.1E-09	3.1E-10	1.9E+00	1.7E-09	1.6E-09	1.1E+01	12.6	23.9	140	5.03	83.4	16.6	Trypsin #2 cells 4mmol Li7
Sample 20	2208	111.1	6.9	2.3	12.0	1.6E-08	1.2E-09	7.3E+00	3.3E-10	3.0E-10	2.1E+00	12.8	93.2	27	0.25	20.0	80.0	Trypsin #2 Cells 4mmol Li6
Sample 21	2209	5.7	49.7	0.5	7.4	8.2E-10	6.2E-11	3.7E-01	7.1E-11	6.5E-11	4.6E-01	138.5	51.7	64	1.06	51.3	48.7	Trypsin #2 Media C
Sample 22	2106	2427.0	2.7	12.1	2.7	3.5E-07	2.7E-08	1.6E+02	1.7E-09	1.6E-09	1.1E+01	135.2	21589	1528	0.06	5.7	94.3	Trypsin #2 Media 4mmol Li6
Sample 22 - rpt	2210	2524.8	5.4	10.0	7.8	3.6E-07	2.8E-08	1.7E+02	1.4E-09	1.3E-09	9.3E+00	135.2	22459	1264	0.05	4.6	95.4	Trypsin #2 Media 4mmol Li6
Sample 23	2211	241.3	4.5	230.8	2.2	3.5E-08	2.6E-09	1.6E+01	3.3E-08	3.1E-08	2.2E+02	174.8	2775	37684	11.64	92.1	7.9	Trypsin #2 Media 4mmol Li7
Sample 24	2212	2.1	42.9	0.4	12.7	3.0E-10	2.3E-11	1.4E-01	6.5E-11	6.0E-11	4.2E-01	10.3	1.4	4.3	2.61	72.3	27.7	C1 - cell lysate
Sample 25	2301	3.9	44.4	0.6	20.1	5.6E-10	4.3E-11	2.6E-01	8.8E-11	8.1E-11	5.7E-01	11.6	3.0	6.6	1.91	65.7	34.3	C1 - media
Sample 26	2302	2.1	49.0	0.4	20.6	3.0E-10	2.3E-11	1.4E-01	5.8E-11	5.3E-11	3.7E-01	10.6	1.5	3.9	2.33	70.0	30.0	C2 - cell lysate
Sample 27	2303	3.6	33.4	2.2	10.1	5.2E-10	4.0E-11	2.4E-01	3.1E-10	2.9E-10	2.0E+00	14.1	3.4	28	7.26	87.9	12.1	C2 - media
Sample 28	2304	86.8	7.7	0.8	4.9	1.3E-08	9.5E-10	5.7E+00	1.2E-10	1.1E-10	7.9E-01	10.8	62	8.6	0.12	10.6	89.4	4mmol lysis buffer 6 - cell lysate
Sample 29	2201	38566.5	29.9	149.5	28.8	5.6E-06	4.2E-07	2.5E+03	2.2E-08	2.0E-08	1.4E+02	13.4	34101	1878	0.05	4.5	95.5	4mmol lysis buffer 6 - media
Sample 29 - rpt	2305	29165.1	1.6	112.1	1.7	4.2E-06	3.2E-07	1.9E+03	1.6E-08	1.5E-08	1.0E+02	13.4	25788	1408	0.05	4.5	95.5	4mmol lysis buffer 6 - media
Sample 30	2306	23.1	7.1	5.0	4.5	3.3E-09	2.5E-10	1.5E+00	7.1E-10	6.6E-10	4.6E+00	10.5	16.0	49	2.61	72.3	27.7	4mmol lysis buffer 7 - cell lysate
Sample 31	2107	1986.0	1.9	1906.0	1.4	2.9E-07	2.2E-08	1.3E+02	2.7E-07	2.5E-07	1.8E+03	12.3	1608	21916	11.68	92.1	7.9	4mmol lysis buffer 7 - media
Sample 31 - rpt	2307	2081.8	42.7	2034.1	42.5	3.0E-07	2.3E-08	1.4E+02	2.9E-07	2.7E-07	1.9E+03	12.3	1686	23389	11.90	92.2	7.8	4mmol lysis buffer 7 - media
Sample 32	2308	19.4	14.1	0.4	8.8	2.8E-09	2.1E-10	1.3E+00	6.1E-11	5.6E-11	3.9E-01	103.9	133	41	0.26	20.8	79.2	8mmol lysis buffer 6 - cell lysate
Sample 33	2111	4782.1	1.5	20.7	1.4	6.9E-07	5.2E-08	3.1E+02	3.0E-09	2.8E-09	1.9E+01	125.3	39415	2426	0.05	5.0	95.0	8mmol lysis buffer 6 - media
Sample 33 - rpt	2309	5092.9	1.6	19.7	1.6	7.3E-07	5.6E-08	3.3E+02	2.8E-09	2.6E-09	1.8E+01	125.3	41977	2312	0.05	4.5	95.5	8mmol lysis buffer 6 - media
Sample 34	2310	3.7	28.2	1.2	6.5	5.4E-10	4.1E-11	2.4E-01	1.7E-10	1.5E-10	1.1E+00	106.5	26.0	116	3.81	79.2	20.8	8mmol lysis buffer 7 - cell lysate
Sample 35	2311	459.0	2.8	435.4	1.2	6.6E-08	5.0E-09	3.0E+01	6.3E-08	5.8E-08	4.1E+02	129.0	3894	52451	11.55	92.0	8.0	8mmol lysis buffer 7 - media
Sample 35 - rpt	2108	406.9	4.6	389.1	1.2	5.9E-08	4.4E-09	2.7E+01	5.6E-08	5.2E-08	3.6E+02	129.0	3451	46871	11.64	92.1	7.9	8mmol lysis buffer 7 - media

RSD = Relative standard deviation
Concentration data between detection limit and ~15 ppb 6-Li and between detection limit and ~1 ppb 7-Li are only semi-quantitative
rpt = replicate

Detection Limit 6Li (high-Li re-run)	6.0	ng/mL	(column C)
Detection Limit 7Li (high-Li re-run)	0.25	ng/mL	(column E)
Detection Limit 6Li (All other samples, including rpt group)	2.6	ng/mL	(column C)
Detection Limit 7Li (All other samples, including rpt group)	0.17	ng/mL	(column E)

Table A-1: Raw ICP-MS Data. *Columns C and E are the detected concentration of ^{6}Li and ^{7}Li respectively. Columns D and F indicate the corresponding relative standard deviations. Columns H-J show conversion of total lithium content into mass-corrected ^{6}Li concentrations. Columns L-N show conversion of total lithium content into mass-corrected ^{7}Li concentrations.Columns Q and R show the dilution corrected ^{6}Li and ^{7}Li concentrations respectively (presented in tables 2-1, 2-2, 2-3). Columns U and V show the % ^{7}Li and % ^{6}Li respectively (shown in figures 2-2 to 2-8). Any sample repeats (column A, - rpt) were performed to ensure that high concentrations of lithium were still within the detection ranges. This raw data was produced and compiled by Dr. Brian Kendall, Dr. Chris Yakymchuk, and Sarah McChaugherty*